RMN con campo magnético ciclado
I Introducción

Esteban Anoardo

Laboratorio de Relaxometría y Técnicas Especiales (LaRTE), Grupo de Resonancia Magnética Nuclear – Facultad de Matemática, Astronomía y Física. Universidad Nacional de Córdoba.

Instituto de Física Enrique Gaviola (CONICET). Córdoba – Argentina.

RMN

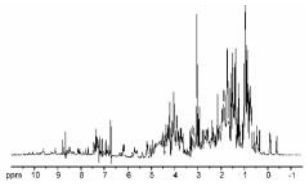

Espectroscopía

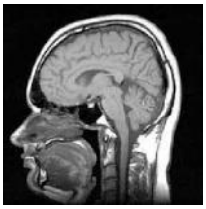

Tomografía

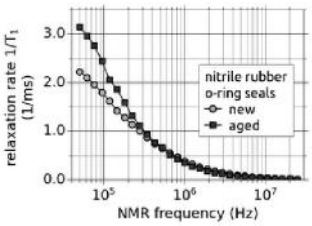

Relaxometría

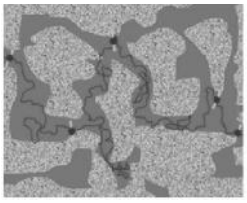

Difusometría

Etc...

¿De qué se trata?

Experimentos de RMN a los cuales se suma la posibilidad de utilizar diferentes valores de campo magnético, en sincronismo con otros eventos destinados a la manipulación espines nucleares y/o electrónicos.

Why magnetic field cycling in NMR experiments?

Signal to noise ratio in NMR experiments

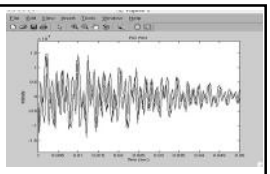

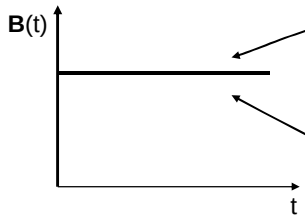

$$S/N \propto B_0 \xi \sqrt{\frac{\eta Q V_s}{k_B T}} \left(\frac{\nu_0}{\Delta \nu}\right),$$

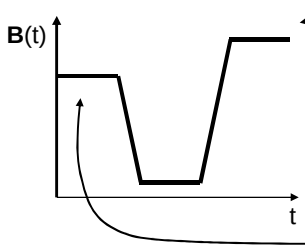

$$S/N \propto B_p \xi \sqrt{\frac{\eta Q V_s}{k_B T}} \left(\frac{\nu_d}{\Delta \nu}\right),$$

Example 1: field-cycling NMR relaxometry

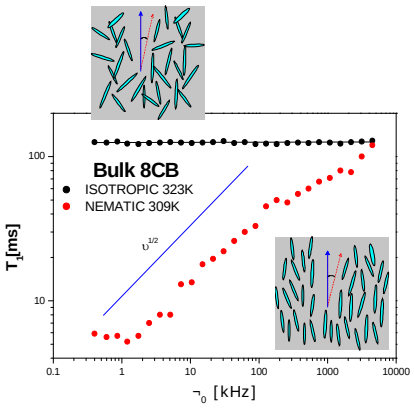

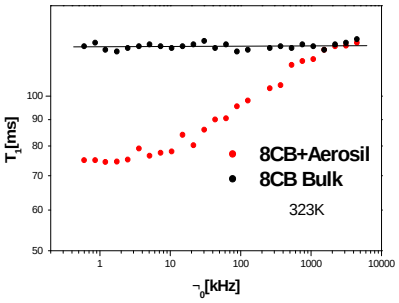

Example 2: nuclear quadrupole double resonance (NQDOR)

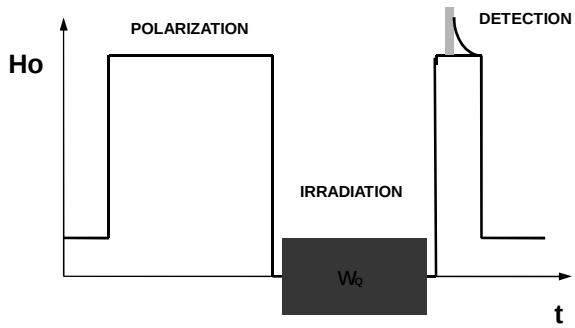

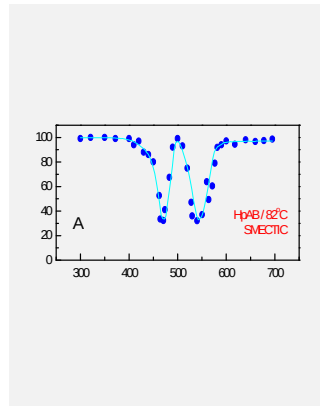

Example 3: zero field NMR

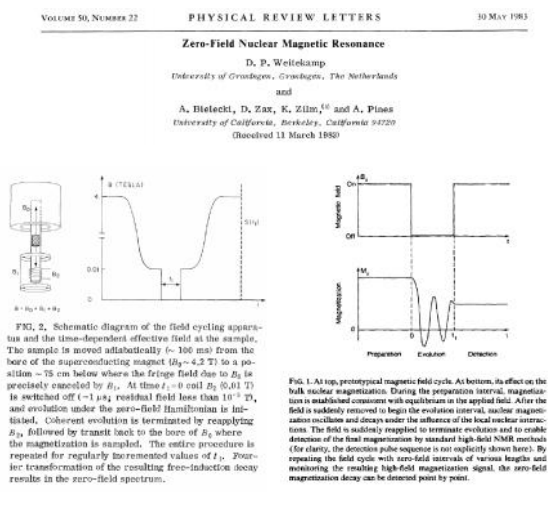

VOLUME 50, NUMBER 22 PHYSICAL REVIEW LETTERS 30 MAY 1983

Zero-Field Nuclear Magnetic Resonance

D. P. Weitekamp
University of Groningen, Groningen, The Netherlands

and

A. Bielecki, D. Zax, K. Zilm,[a] and A. Pines
University of California, Berkeley, California 94720

(Received 11 March 1983)

FIG. 2. Schematic diagram of the field cycling apparatus and the time-dependent effective field at the sample. The sample is moved adiabatically (~ 100 ms) from the bore of the superconducting magnet ($B_0 \sim 4.2$ T) to a position ~ 75 cm below where the fringe field due to B_0 is precisely canceled by B_1. At time $t_1 = 0$ coil B_2 (0.01 T) is switched off (~1 μs; residual field less than 10^{-3} T), and evolution under the zero-field Hamiltonian is initiated. Coherent evolution is terminated by reapplying B_2, followed by transit back to the bore of B_0 where the magnetization is sampled. The entire procedure is repeated for regularly incremented values of t_1. Fourier transformation of the resulting free-induction decay results in the zero-field spectrum.

FIG. 1. At top, prototypical magnetic field cycle. At bottom, its effect on the bulk nuclear magnetization. During the preparation interval, magnetization is established consistent with equilibrium in the applied field. After the field is suddenly removed to begin the evolution interval, nuclear magnetization oscillates and decays under the influence of the local nuclear interactions. The field is suddenly reapplied to terminate evolution and to enable detection of the final magnetization by standard high-field NMR methods (for clarity, the detection pulse sequence is not explicitly shown here). By repeating the field cycle with zero-field intervals of various lengths and monitoring the resulting high-field magnetization signal, the zero-field magnetization decay can be detected point by point.

FIG. 1. Proton NMR spectra of barium chlorate hydrate [$Ba(ClO_3)_2 \cdot H_2O$]. All H_2O proton-proton vectors are coparallel in the unit cell. (a) High-field powder spectrum showing normal broadened Pake doublet. (b) High-field single-crystal spectrum. The sample is oriented in an arbitrary direction. The observed splitting depends on both intermuclear distance and orientation. (c) Zero-field powder spectrum. The major features are those predicted by the simple treatment given in the text for a pair of coupled spins of $\frac{1}{2}$. The observed splitting is a direct, orientation-independent measure of the intermuclear distance. The central peak arises from spins in crystallite orientations which did not evolve in zero field.

Example 4: electron-nuclear double resonance (ENDOR)

Detection of Anisotropic Hyperfine Transitions in Zero Magnetic Field Using Field-Cycling Techniques

G. Sturm, D. Kilian, A. Lötz,[1] and J. Voitländer
Institut für Physikalische Chemie, Universität München, Butenandtstraße 5-13, D-81377 Munich, Germany

Journal of Magnetic Resonance **142**, 139–144 (2000)

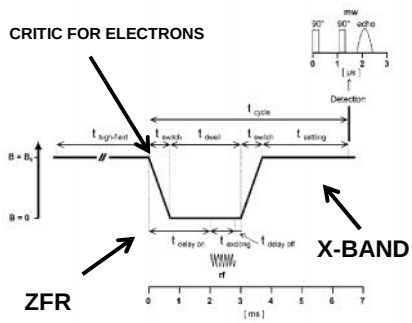

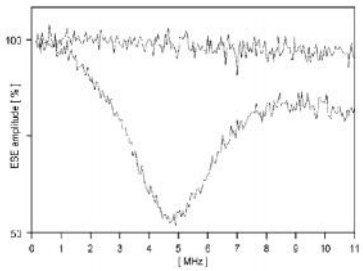

FIG. 2. Pulsed field-cycled ENDOR spectrum of a coal sample at 4.2 K obtained with our old field-cycling solenoid (see text). Echo intensity versus RF irradiation frequency in MHz. Two low-power microwave pulses of 300 as length were used for the detection. (Bottom) Recovered EPR amplitude after irradiation in zero field. No accumulation. (Top) Equal experimental conditions, yet without RF irradiation. Experimental parameters: $t_{high\text{-}field} = 2$ s, $t_{switch} = 0.5$ ms, $t_{delay\ on} = 0.5$ ms, $t_{excitation} = 0.8$ ms, $t_{delay\ off} = 0.2$ ms, $t_{settling} = 2$ ms.

Quadrupole dips

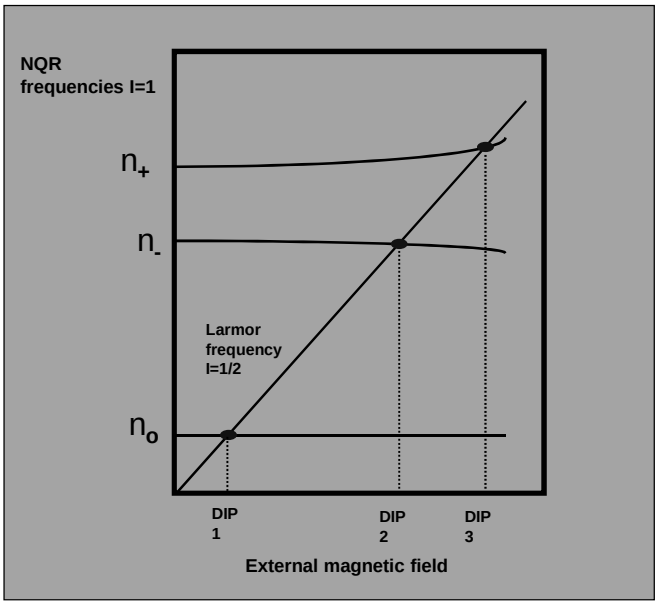

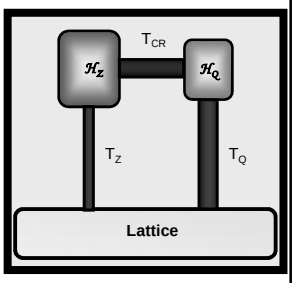

Example 5: field-cycling MRI

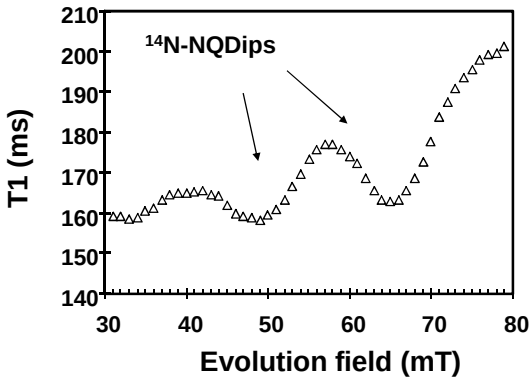

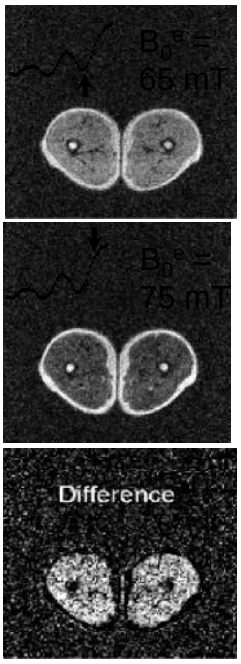

Data acknowledged to David Lurie (Aberdeen)

Pregunta: ¿es posible pensar en una sola máquina que permita realizar todos estos experimentos?

III Relaxometría

Relaxometría: *dependencia de un parámetro de relajación magnética nuclear o electrónico con una o más escala/s de tiempo/s determinada/s*

Ejemplos: T_1, T_2, T_{1r}, T_{1D}, T_{1Q}, T_D, T_{2r}, T_{2e}, *etc.*

$$\nu_0 = \gamma . B / 2 \pi$$

También llamada “espectroscopía de relajación en el pasado”

Escalas de tiempos:

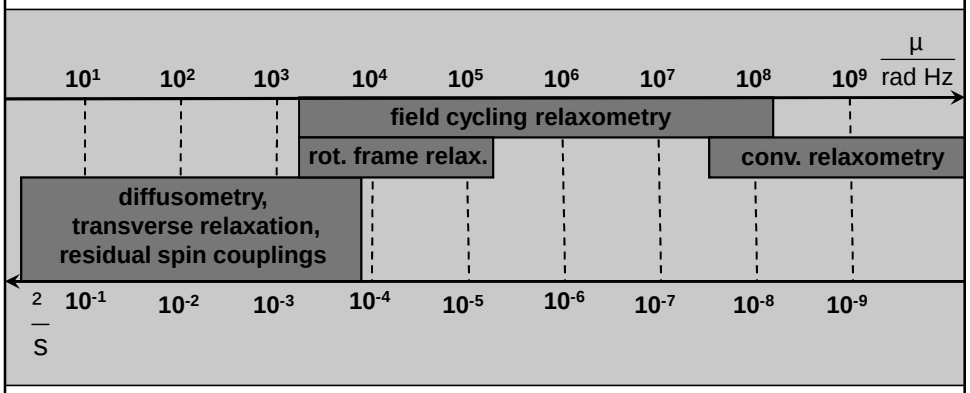

Experimento básico: ***dependencia de T1 (relajación espín-red) con la frecuencia de Larmor***

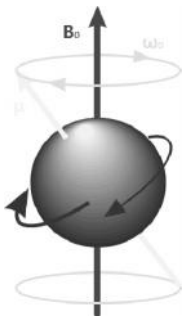

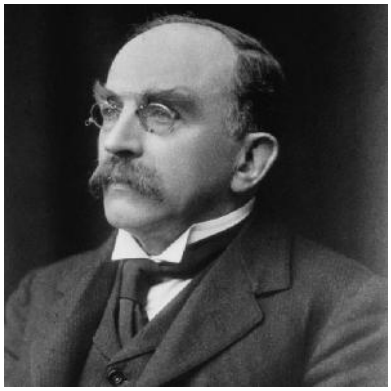

Fundamentos

⇨ Mecanismos de relajación

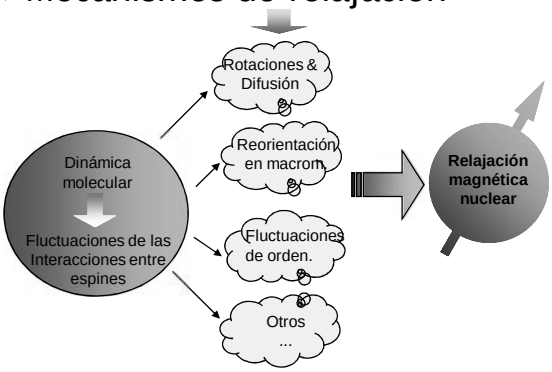

Tiempo de relajación longitudinal T_1

- **Existencia de un acople entre el sistema de espines y el medio que lo rodea (red).**
- **El sistema de espines es perturbado (ej.: pulso de RF) y éste regresa al equilibrio termodinámico con el campo magnético en el cual se encuentra (Ley de Curie).**

Transiciones entre niveles de energía del sistema de espines ⇨ **Transiciones entre niveles de energía del espectro dinámico**

Modelo fenomenológico: ***ecuaciones de Bloch***

$$\frac{dM_x}{dt} = \gamma\,(M_y B_0 + M_z B_1 \sin\omega t) - \frac{M_x}{T_2}$$

$$\frac{dM_y}{dt} = \gamma\,(M_z B_1 \cos\omega t + M_x B_0) - \frac{M_y}{T_2}$$

$$\frac{dM_y}{dt} = \gamma\,(-M_x B_1 \sin\omega t - M_y B_1 \cos\omega t) - \frac{(M_z - M_0)}{T_1}$$

Modelo

⇨ Formalismo

➢**Hamiltoniano de interacciones de espines:**

$$H_i(t) = f_i \sum_k F^{(k)}(t)\ \mathbf{O}^{(k)}$$

Donde:

f_i : constantes dependientes del tipo de interacción

$F^{(k)}(t)$: fluctuaciones de la red (función)

$\mathbf{O}^{(k)}$: operador de espín

Normalización:: $G(0) = \frac{1}{2\pi}\int_{-\infty}^{\infty} J(\mu)\ d\mu = 1$

➢**Función de autocorrelación reducida:**

$$G(\tau) = \frac{\left\langle F^{(k)}(0)\ F^{(-k)}(\tau)\right\rangle_{ensemble}}{\left\langle \left|F^{(k)}\right|^2\right\rangle_{ensemble}}$$

Fluctuaciones estocásticas del campo local producido por los vecinos genera relajación.

La función de correlación nos indica el grado de correlación que tendrá la perturbación local en un tiermpo posterior.

Densidad espectral: $J(\mu) = \int_{-\infty}^{\infty} G(\tau)\ e^{-i\mu\tau}\ d\tau$

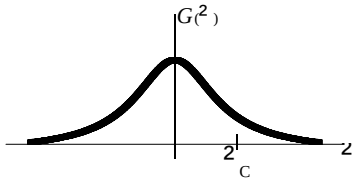

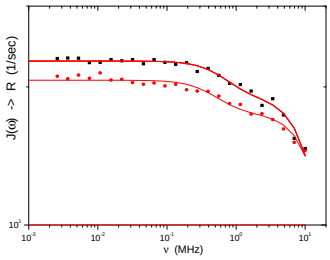

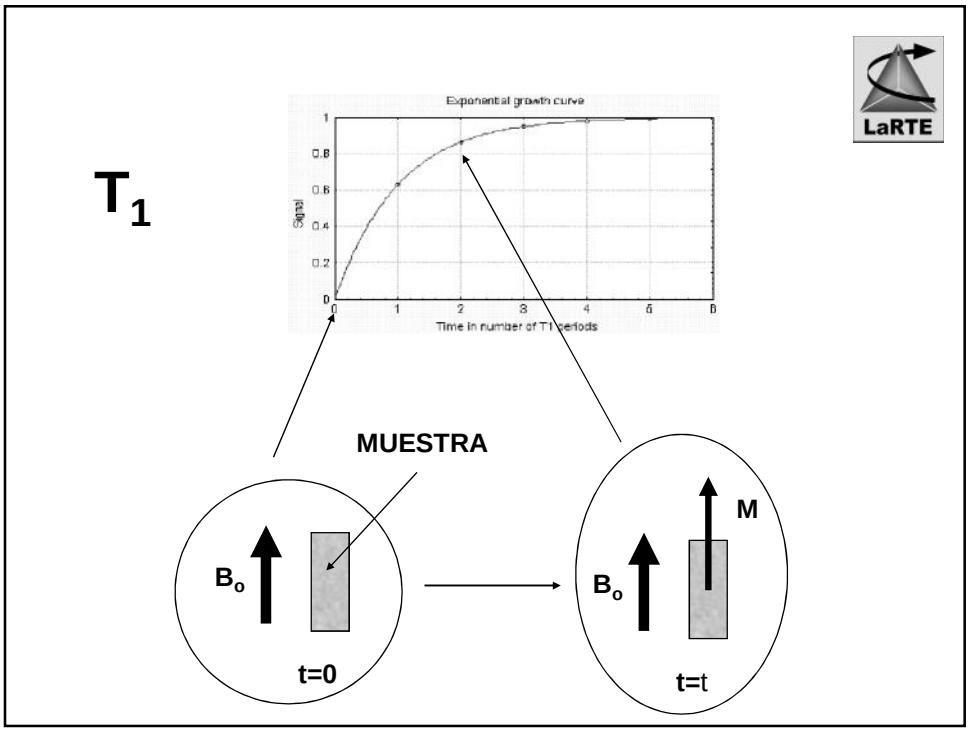
T1
Exponential growth curve
Signal
Time in number of T1 periods
MUESTRA
Bo
t=0
M
Bo
t=t

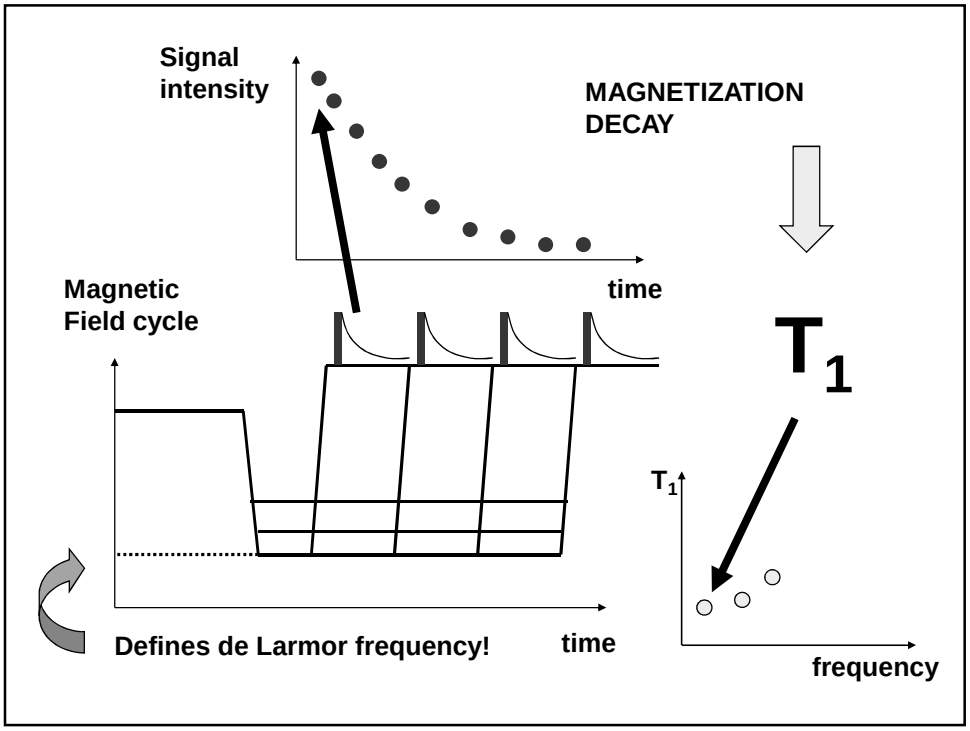
Signal intensity
MAGNETIZATION DECAY
time
Magnetic Field cycle
T1
T1
Defines de Larmor frequency!
time
frequency

What do we measure?

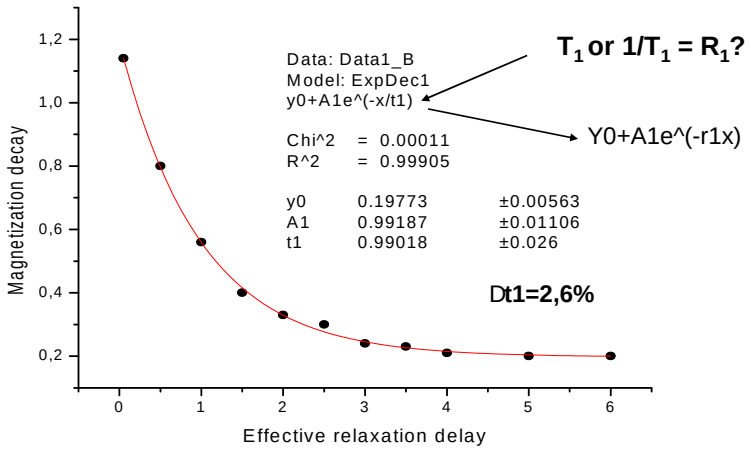

T_1 or $1/T_1 = R_1$?

Y0+A1e^(-r1x)

About the magnetic field sequence

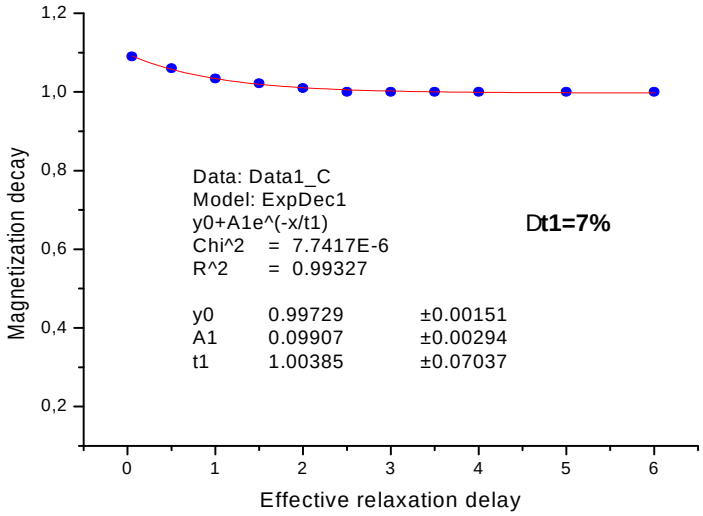

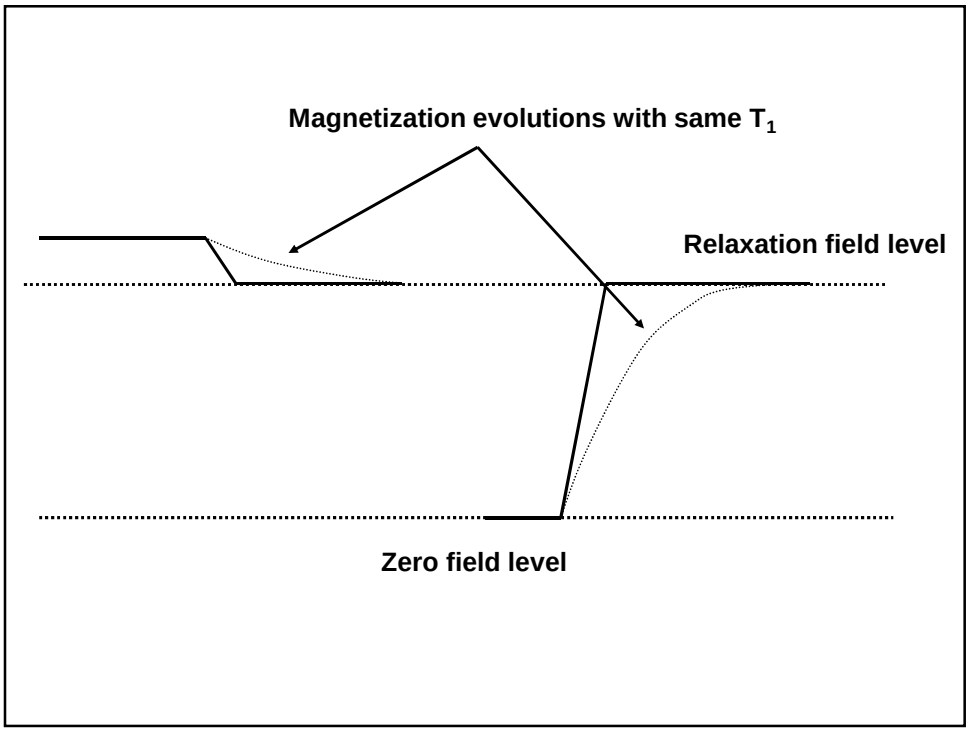
Magnetization evolutions with same T_1
Relaxation field level
Zero field level

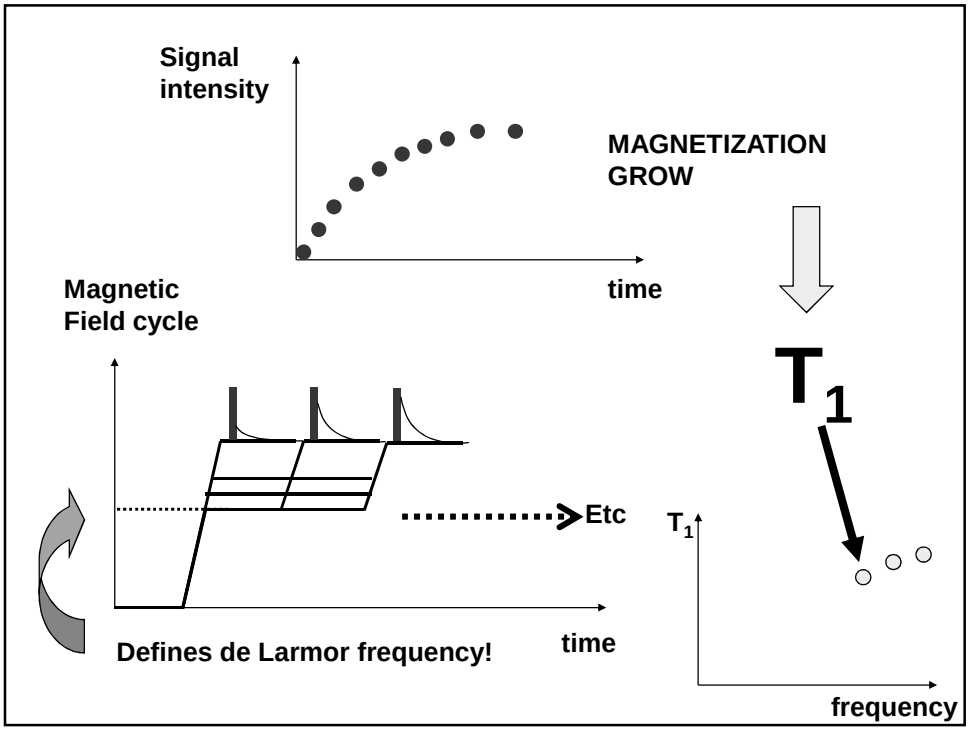
Signal intensity
MAGNETIZATION GROW
time
Magnetic Field cycle
T_1
Etc
T_1
Defines de Larmor frequency!
time
frequency

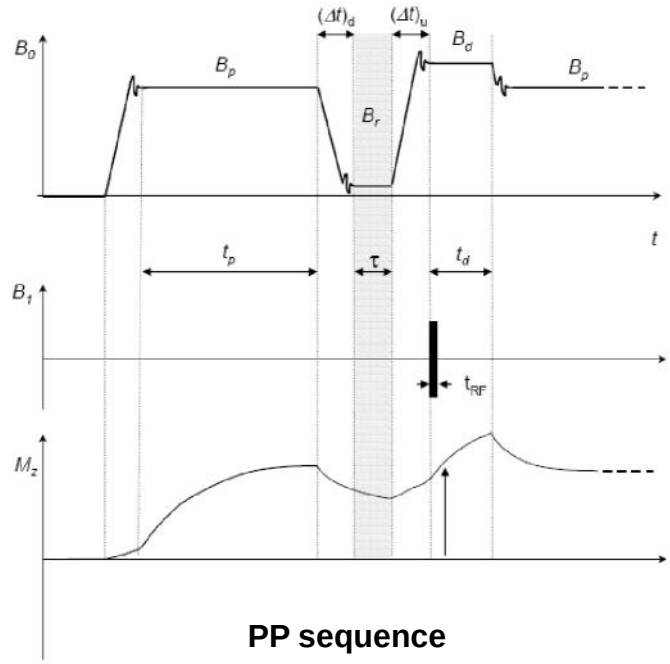

PP sequence

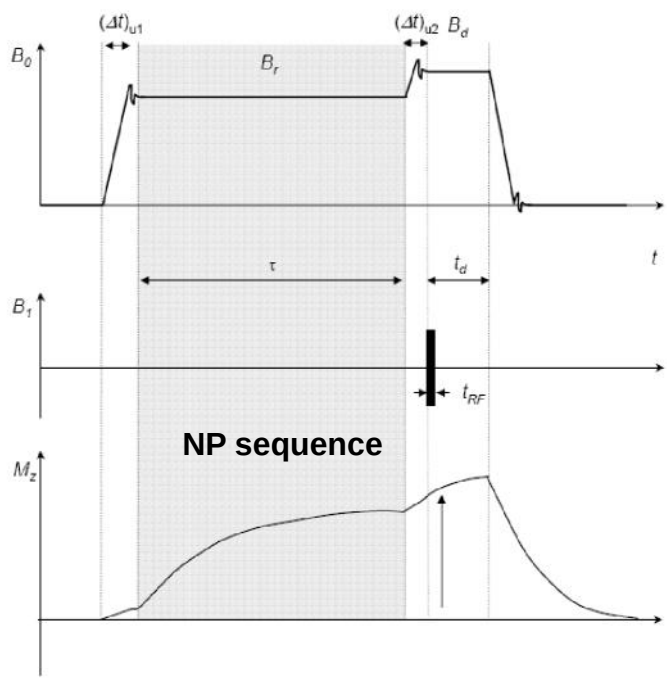

NP sequence

Switching times

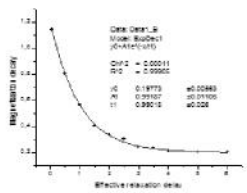

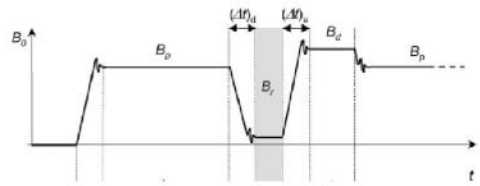

$$M_z(\tau) = M_0(B_r) + [M_0(B_p) - M_0(B_r)]\exp\{-\tau/T_1(B_r)\}.$$

$$M_z[\tau + (\Delta t)_d + (\Delta t)_u]$$
$$= [(M_z[(\Delta t)_d] - M_0^r)e^{-\tau/T_1(B_r)} + M_0^r]e^{-c_1^u} + c_2^u,$$

$$M_z^{\text{detected}}(\tau) = M_z^{\infty} + \Delta M_z^{\text{eff}} e^{-\tau/T_1},$$

Glossary

- T_1 relaxation dispersion [s]
- T_1 profile
- Relaxation rate ($1/T_1$ or R_1) dispersion [s^{-1}]
- NMRD: nuclear magnetic relaxation dispersion
- NMRD profile

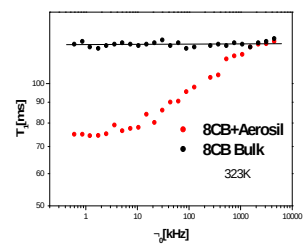

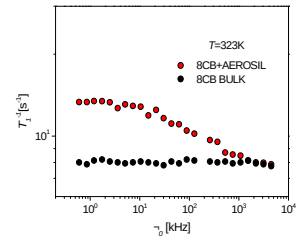

Relaxivity: relaxation rate for a given concentration in a solution [mM^{-1} s^{-1}]

Preguntas

1. ¿Con que criterio utilizo secuencia PP o NP?

2. ¿Qué cuidados debo tener para regular el ciclo útil del experimento en cada caso?

IV- Cristales líquidos

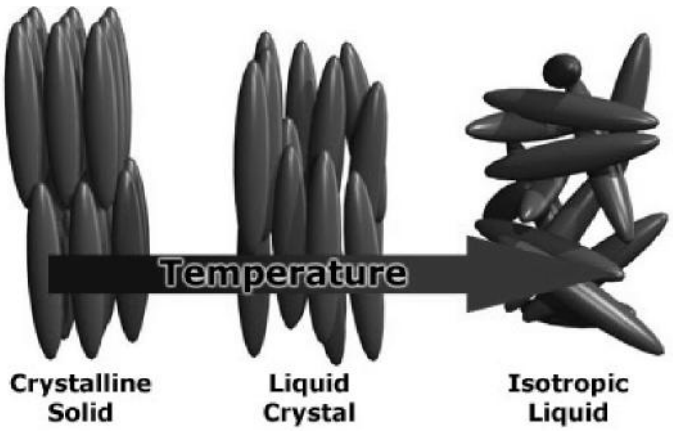

Common thermotropic mesophases

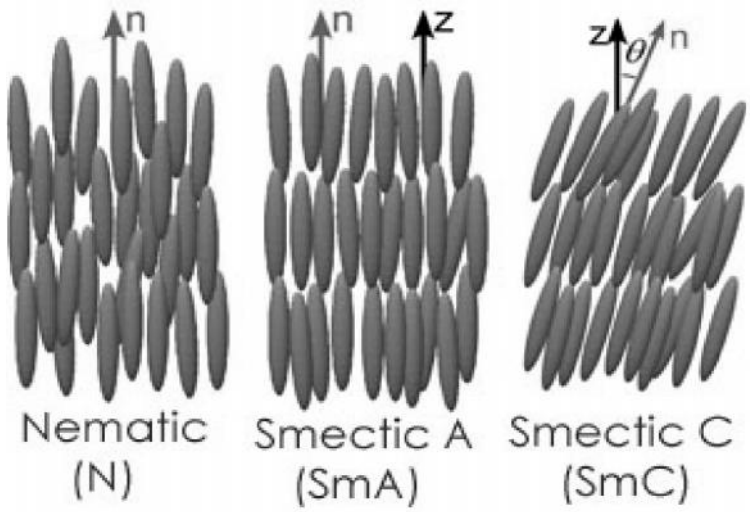

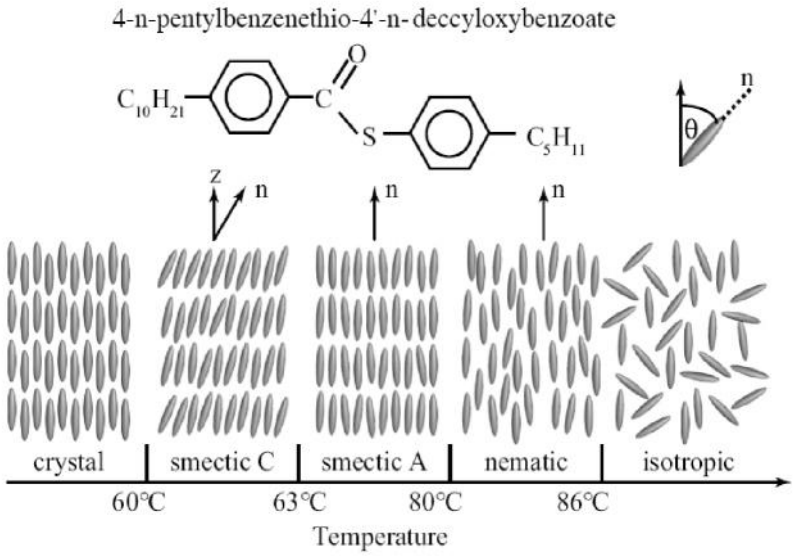

Source: *Liquid Crystals: frontiers in biomedical applications. G. P. Crawford and F. J. Woltman*

- **5CB: 4-cyano-4'-5-alkylbiphenil**

Cry-N	N-Iso
24C	35.3C

- **8CB: 4-cyano-4'-8-alkylbiphenil**

Cry-SmA	SmA-N	N-Iso
21.5C	33.5C	40.5C

- **11CB: 4-cyano-4'-11-alkylbiphenil**

Cry-SmA	SmA-Iso
53C	57.5C

Cyanobiphenyl homologous series: transition temperatures

Chain length	Abbreviation	Transitions
$n = 5$	(5CB)	N $\leftrightarrow$ 35°C $\leftrightarrow$ I
$n = 6$	(6CB)	N $\leftrightarrow$ 38°C $\leftrightarrow$ I
$n = 7$	(7CB)	N $\leftrightarrow$ 42°C $\leftrightarrow$ I
$n = 8$	(8CB)	SmA $\leftrightarrow$ 33.3°C $\leftrightarrow$ N $\leftrightarrow$ 38°C $\leftrightarrow$ I
$n = 9$	(9CB)	SmA $\leftrightarrow$ 48.3°C $\leftrightarrow$ N $\leftrightarrow$ 49.7°C $\leftrightarrow$ I
$n = 10$	(10CB)	SmA $\leftrightarrow$ 50.7°C $\leftrightarrow$ I
$n = 11$	(11CB)	SmA $\leftrightarrow$ 52.7°C $\leftrightarrow$ I
$n = 12$	(12CB)	SmA $\leftrightarrow$ 56.9°C $\leftrightarrow$ I

Source: *Liquid Crystals: frontiers in biomedical applications. G. P. Crawford and F. J. Woltman*

Molecular dynamics

NMR Relaxation

Molecular order

Solid State Communications, Vol. 7, pp. 415–417, 1969. Pergamon Press. Printed in Great Britain

NUCLEAR RELAXATION IN A NEMATIC LIQUID CRYSTAL

P. Pincus*

Laboratoire de Physique des Solides†, Faculté des Sciences, 91 Orsay, France

We estimate the contributions to T_1 and T_2 in a nematic liquid crystal arising from the fluctuations in the orientational order. This results in relaxation times of the order of one second which is typical of ordinary liquids. There is however an additional striking dependence on the nuclear resonance frequency, $T_1 \propto \omega^{1/2}$

For a given wavevector $\mathbf{q}$ and polarization α, one finds two relaxation modes, one mainly hydrodynamic and the other mainly orientational. For these latter modes (of interest here) the relaxation spectrum is:

$$i\omega(q) \approx i(Kq^2 + \chi H^2)/\eta, \qquad (7)$$

$$J(\omega) = \int_{-\infty}^{\infty} G(t)\, e^{-i\omega t}\, dt,$$

$$G(t) = \langle \delta n^-(0)\, \delta n^+(t) \rangle$$

If we boldly assume that the orientational and diffusive motions are uncoupled, the correlation function may be written:

$$G(t) = (2\pi)^{-3} \int d\mathbf{q} \left(\frac{k_B T}{K q^2}\right) e^{-(K/\eta)q^2 t}\, e^{-Dq^2 t} \qquad (8)$$

where D is the diffusion constant, $D = k_B T/6\pi a\eta$ (a is a molecular dimension).

we find:

$$1/T_1 = \omega_D^2 t_c$$

where ω_D is a dipolar frequency and the correlation time t_c is given by:

$$t_c = \frac{3}{2}\frac{k_B T}{K}\left(\langle n_0^2 \rangle - \frac{1}{3}\right)[\omega(D + K/\eta)]^{-1/2}$$

5. Orsay Liquid Crystal Group, Submitted for Publication in *J. chem. Phys.*

VOLUME 23, NUMBER 17 PHYSICAL REVIEW LETTERS 27 OCTOBER 1969

SPIN RELAXATION AND SELF-DIFFUSION IN LIQUID CRYSTALS*

R. Blinc,† D. L. Hogenboom,‡ D. E. O'Reilly, and E. M. Peterson
Argonne National Laboratory, Argonne, Illinois 60439
(Received 6 August 1969)

The frequency and temperature dependence of proton relaxation times have been measured for the nematic liquid-crystal and isotropic liquid phases of *p*-azoxyanisole and *p*-azoxyphenetole as well as for the "neat" mesophase of sodium stearate. Self-diffusion coefficients were determined by the proton-spin-echo method. The anomalous effects found are interpreted in terms of collective long-range-order fluctuations in the nematic region and a residual order in the isotropic liquid.

$8\pi^3$. Equation (9) reduces in the limit $r \ll \omega_0$ to the result given by Pincus,[3]

$$J^{(1)}(\omega_0) \propto \omega_0^{-1/2}, \qquad \text{where } r = \Delta\chi H_0^2/\eta$$

From the well-known expressions[7] for T_1 and $T_{1\rho}$ one obtains

$$T_1^{-1} = \tfrac{2}{5} T_{1\rho}^{-1} = \frac{9\gamma^4\hbar^2}{8R^6} J^{(1)}(\omega_0). \qquad (10)$$

Frequency Dependence of Proton Spin Relaxation in Liquid Crystalline PAA

W. Wölfel, F. Noack and M. Stohrer
Physikalisches Institut der Universität Stuttgart

(Z. Naturforsch. 30a, 437–441 [1975]; received February 11, 1975)

We report on measurements of the Larmor frequency dependence of the proton spin relaxation time T_1 in the nematic and isotropic phase of p-azoxyanisole (frequency range: 3.8 kHz $\leq \omega_L/2\pi \leq$ 75 MHz). In both cases our results clearly support the Pincus-Cabane mechanism of spin relaxation by order fluctuations ("$\omega_L^{-1/2}$-law") and exclude the alternative translational diffusion model ("$\omega_L^{+1/2}$-law"). For the isotropic phase it was possible to evaluate the correlation time τ of the liquid crystalline order fluctuations from the observed T_1 dispersion. As a function of the deviation $\Delta\vartheta = \vartheta - \vartheta_c$ from the critical nematic-isotropic transition temperature, $\vartheta_c = (136 \pm 0.5)$ °C, we found $\tau = 2.71 \cdot 10^{-7} \cdot \Delta\vartheta^{-0.25}$ s.

Dispersion law predicted by P. Pincus in 1969

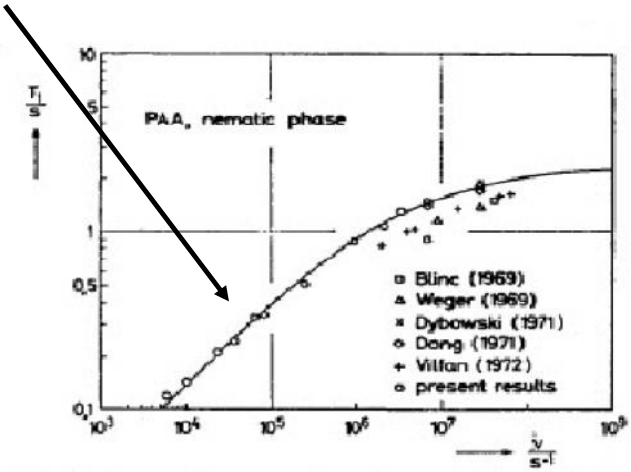

Fig. 1. Larmor frequency dependence of the longitudinal proton spin relaxation time T_1 in the nematic phase of PAA at a temperature $\vartheta = 123.5$ °C. Points: Experimental results from this work (○); from Ref. 3 a (□); from Ref. 3 b (△); from Ref. 3 g (×); from Ref. 3 i (◇); from Ref. 3 k (+). Full curve: Computer fit of the Pincus model, Eq. (1), to (○); $A = 0.431\ s^{-1}$, $B = 673.7\ s^{-3/2}$.

LIQUID CRYSTALS, 1988, VOL. 3, NOS. 6 AND 7, 907–925

Invited Article

Relaxation dispersion and zero-field spectroscopy of thermotropic and lyotropic liquid crystals by fast field-cycling N.M.R.

by F. NOACK, M. NOTTER and W. WEISS
Physikalisches Institut der Universität Stuttgart, Pfaffenwaldring 57, 7000 Stuttgart 80, F.R. Germany

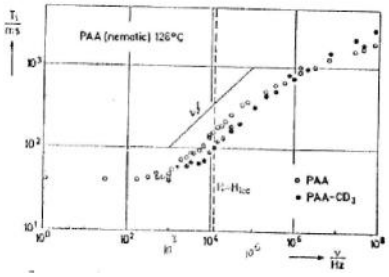

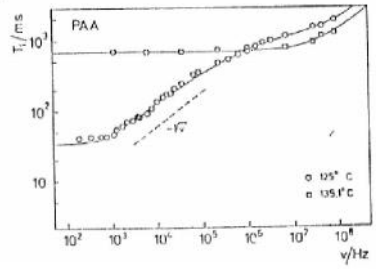

T_1 relaxation driven by ODF

$$T_1^{-1} = f(J_1(\omega), J_2(\omega))$$

$$J_K(\mu) = \mathrm{Re}\int_{-\infty}^{\infty} G_K(\tau) e^{-i\mu\tau}\, d\tau$$

K=1,2

$$G_K = \left\langle Y_{2K}(0) Y_{2K}^{*}(\tau) \right\rangle$$

$$Y_{2K} = g[\Omega(\tau), \gamma(\tau)]$$

If **n** fluctuates around **B:**

$$Y_{21} \propto \Omega \ldots\ldots Y_{22} \propto \Omega^2$$

$$G_1(\tau) = \left\langle n_x(\mathbf{r},t) n_x(\mathbf{r},t+\tau) \right\rangle + \left\langle n_y(\mathbf{r},t) n_y(\mathbf{r},t+\tau) \right\rangle$$

Elastic and magnetic free energy

$$G_1(\tau) = \frac{3}{2}\sum_{q,q'} \left\{ \left\langle n_1(\mathbf{q},t).n_1^{*}(\mathbf{q}',t+\tau) \right\rangle \left\langle n_2(\mathbf{q},t).n_2^{*}(\mathbf{q}',t+\tau) \right\rangle \right\}$$

n_1:splay+bend n_2:twist

$$F = \frac{1}{2}\left\{ K_{11}(\nabla.\mathbf{n})^2 + K_{22}(\mathbf{n}.\nabla \wedge \mathbf{n})^2 + K_{33}(\mathbf{n} \wedge \nabla \wedge \mathbf{n})^2 \right\}$$

Magnetic "orienting" term:

$$F_m = -\frac{1}{2}\frac{\Delta\chi}{\mu_0}(\mathbf{n}.\mathbf{B})^2$$

$$F = \frac{1}{2V}\sum_{\mathbf{q}}\sum_{\alpha=1}^{2} K_\alpha(\mathbf{q}) \left| \mathbf{n}_\alpha(\mathbf{q}) \right|^2$$

$$K_\alpha = K_{\alpha\alpha} q_\perp^2 + K_{33} q_\parallel^2 + \frac{\Delta\chi}{\mu_0} B^2$$

The nematic ODF relaxation mechanism

1 $\left\langle n_{\sim}(\mathbf{q})\, n_{\sim}^{*}(\mathbf{q}')\right\rangle = \delta_{qq'} \left\langle \left| n_{\sim}(\mathbf{q}) \right|^{2} \right\rangle$

2 $\frac{\partial}{\partial t} n_{\sim}(\mathbf{q}) = -\frac{1}{\tau_{\sim}(\mathbf{q})} n_{\sim}(\mathbf{q})$ $\quad \tau_{\sim}(\mathbf{q}) = \frac{\eta_{\sim}(\mathbf{q})}{K_{\sim}(\mathbf{q})}$

3 $K_{11} = K_{22} = K_{33}$ $\quad \sim = 1,2$

4 $K_{\sim} \approx K q^{2}$

$$J_1(\mu) \propto \mu^{-\frac{1}{2}}$$

Pincus – Blinc (1969)

Rotating-frame spin-lattice relaxation: $T_{1\rho}$

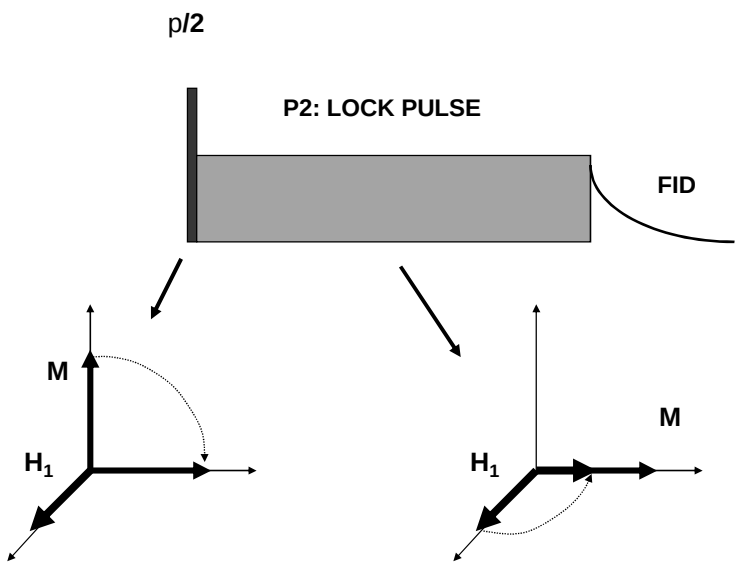

Differences between rotating and laboratory-frame spin-lattice relaxation

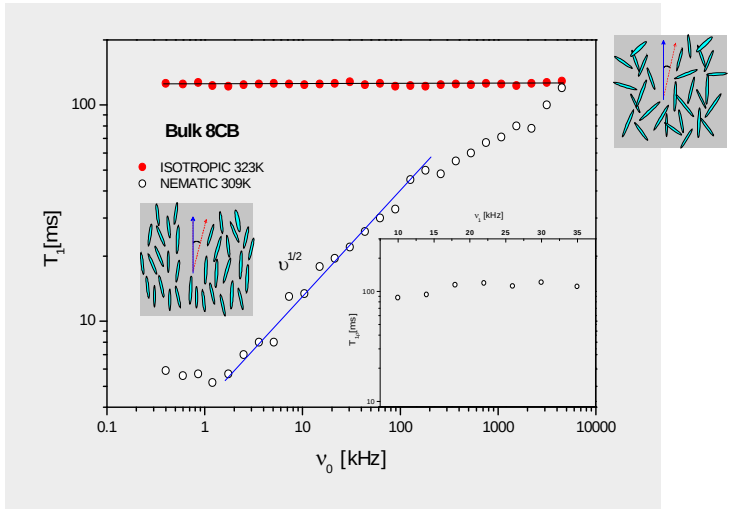

$$J_K(\mu) = \mathrm{Re}\int_{-\infty}^{\infty} G_K(\tau)e^{-i\mu\tau}\,d\tau$$

$$G_K = \langle Y_{2K}(0)Y_{2K}^*(\tau)\rangle$$

$$Y_{2,0}(t) = \sqrt{\frac{5}{16\pi}}(3\cos^2\vartheta(t) - 1),$$

$$Y_{2,1}(t) = -\sqrt{\frac{15}{8\pi}}\sin\vartheta(t)\cos\vartheta(t)\exp(i\varphi(t)),$$

$$Y_{2,2}(t) = \sqrt{\frac{15}{32\pi}}\sin^2\vartheta(t)\exp(2i\varphi(t)).$$

$$Y_{2,0}(t) \simeq \sqrt{\frac{5}{16\pi}}\left(2 - 3\vartheta'^2 + \frac{3}{4}\vartheta'^4\right) \simeq \frac{1}{2}\sqrt{\frac{5}{\pi}},$$

$$Y_{2,1}(t) \simeq -\sqrt{\frac{15}{8\pi}}\vartheta'\left(1 - \frac{2}{3}\vartheta'^2 + \frac{1}{12}\vartheta'^4\right)\exp(i\varphi') \simeq -\sqrt{\frac{15}{8\pi}}\vartheta'\exp(i\varphi'),$$

$$Y_{2,2}(t) \simeq \sqrt{\frac{15}{32\pi}}\vartheta'^2\left(1 - \frac{1}{3}\vartheta'^2 + \frac{1}{36}\vartheta'^4\right)\exp(2i\varphi') \simeq \sqrt{\frac{15}{32\pi}}\vartheta'^2\exp(2i\varphi').$$

Small angle fluctuations

$$\frac{1}{T_1(\omega_0)} = K[J_1(\omega_0) + 4J_2(2\omega_0)],$$

$$\frac{1}{T_{1\rho}(\omega_1,\omega_0)} = \frac{K}{2}[3J_0(2\omega_1) + 5J_1(\omega_0) + 2J_2(2\omega_0)],$$

$$\frac{1}{T_{1\rho}(\omega_1)} = \frac{3K}{2}[J_0(2\omega_1) + \alpha],$$

Smectic A phase

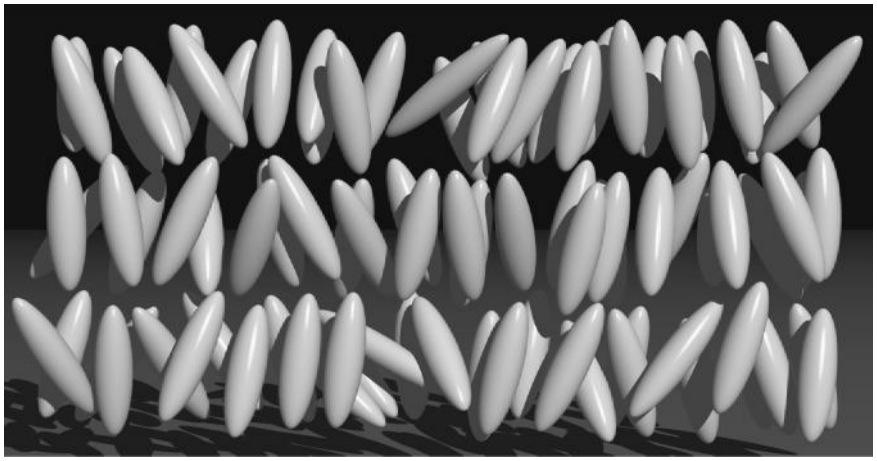

The Journal of Chemical Physics, Vol. 63, No. 8, 15 October 1975

Proton spin–lattice relaxation in smectic TBBA

R. Blinc*

Solid State Physics Laboratory, ETH, CH-8049 Zürich, Switzerland

M. Luzar, M. Vilfan, and M. Burgar

University of Ljubljana, J. Stefan Institute, Ljubljana, Yugoslavia
(Received 28 April 1975)

Another possible relaxation mechanism is the *contribution of the smectic undulation waves*,[5] when the interlayer distance is kept constant and the directors are normal to the layers. The relation between the local

Using the elastic continuum theory,[5] it can be easily shown that for $\omega \ll \omega_c$ the spectral density $I_h(p\omega)$ becomes

$$I_h(p\omega) = f_h(\Delta) \cdot S^2 \cdot \frac{kT}{4 \cdot K_1 \cdot \xi} \cdot \frac{1}{p\omega} , \qquad (12)$$

where ξ is a coherence length in the z direction, i.e., the z dimension of the part of the sample where the smectic layers are parallel to each other.

Investigation of Molecular Motion in Smectic Phases of the Liquid Crystal TBBA by NMR Relaxation Dispersion

Th. Mugele, V. Graf, W. Wölfel, and F. Noack
Physikalisches Institut der Universität Stuttgart

Z. Naturforsch. 35a, 924–929 (1980); received July 7, 1980

of smectic phases. Since 1975 the pioneering works in the field have been performed by Blinc et al. [1], who transferred the basic ideas of the well-established relaxation models for nematics to smectics and

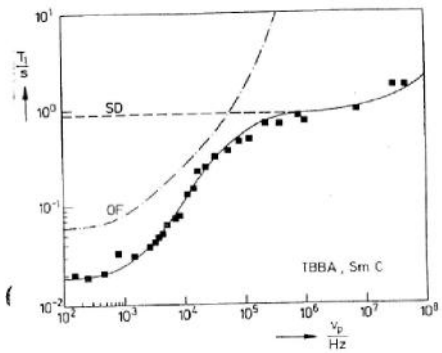

simulation). At first sight the model used seems quite satisfactory; however, the analysis has to be rejected because it fails certainly to yield diffusion constants in accordance with more direct measure-

To overcome the problem with the incorrect value of D, we extended (1) by a third term, T_{1x}^{-1}, which for simplicity was assumed to possess a Debye-like power spectrum (parameters: amplitude factor A_x; correlation time τ_x) as a first approximation to any type of molecular reorientation open to discussion, e.g. rotational motions or other order fluctuation mechanisms that are not included in (1).

J. Chem. Phys. 86 (2), 15 January 1987

Nuclear spin relaxation due to order director fluctuations in the smectic *A* phase

M. Vilfan, M. Kogoj, and R. Blinc
J. Stefan Institute, E. Kardelj University of Ljubljana, 61111 Ljubljana, Yugoslavia

Since 1969 a number of studies have been devoted to nuclear spin relaxation in the smectic *A* phase.[1-8] By now strong evidence exists that collective modes, similar to nematic order director fluctuations, persist in the smectic *A* mesophase giving rise to a relaxation rate $(T_1^{-1})_{OF}$ proportional to the inverse square root of the Larmor frequency ω_L. However, at low frequencies a deviation from this behavior has been observed.[3,5] The leveling off of the dispersion curve was ascribed by some authors to the influence of the smectic order parameter,[3,9] and by others formally to the lack of the ultralong wavelength elastic deformations which cannot exceed the dimension of a uniformly oriented domain ("low frequency cutoff").[5]

$$J_1(\omega_L) = S^2 r^{-6} \operatorname{Re} \int_{-\infty}^{\infty} \langle \delta\mathbf{n}(\mathbf{r},0)\cdot\delta\mathbf{n}(\mathbf{r},t)\rangle e^{i\omega_L t} dt .$$

$$J_1(\omega_L) = \frac{S^2 k T r^{-6} \eta}{4\pi^2 K_1^{3/2}\sqrt{B}} \times \ln \frac{q_{zc} + \left[q_{zc}^2 + (\omega_L \eta/2\sqrt{K_1 B})^2\right]^{1/2}}{\omega_L \eta/(2\sqrt{K_1 B})}, \quad (10)$$

this phase. Definite conclusions about it cannot be made at present in view of the indefinitiveness concerning the relative importance of two competing relaxation mechanisms in the MHz region in the smectic *A* phase of liquid crystals, i.e., of order fluctuations on one side and molecular self-diffusion on the other. Molecular self-diffusion gives namely—taken

where q_{zc} denotes the upper limit of the component of wave vector in the direction perpendicular to the smectic layers, while the upper limit of $q_\perp$ is taken ∞. $J_1(\omega_L)$ calculated within this model would diverge for $q_{zc} \to \infty$. The existing experimental data are not in agreement with the logarithmic frequency dispersion as predicted by Eq. (10).

Typical dispersion for Smectic A

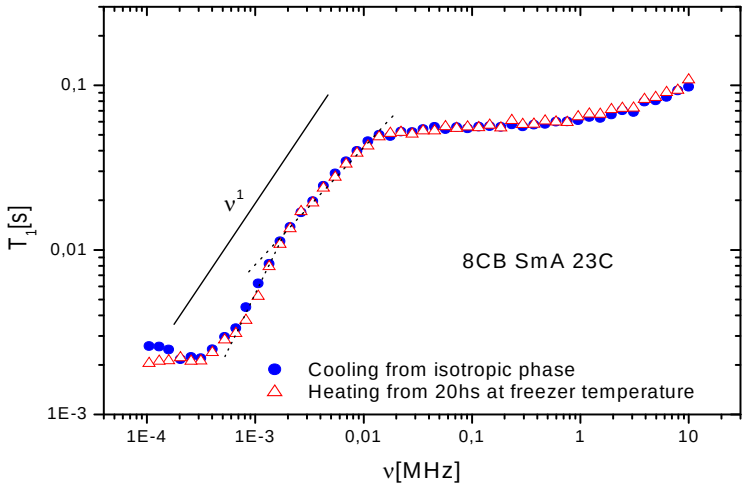

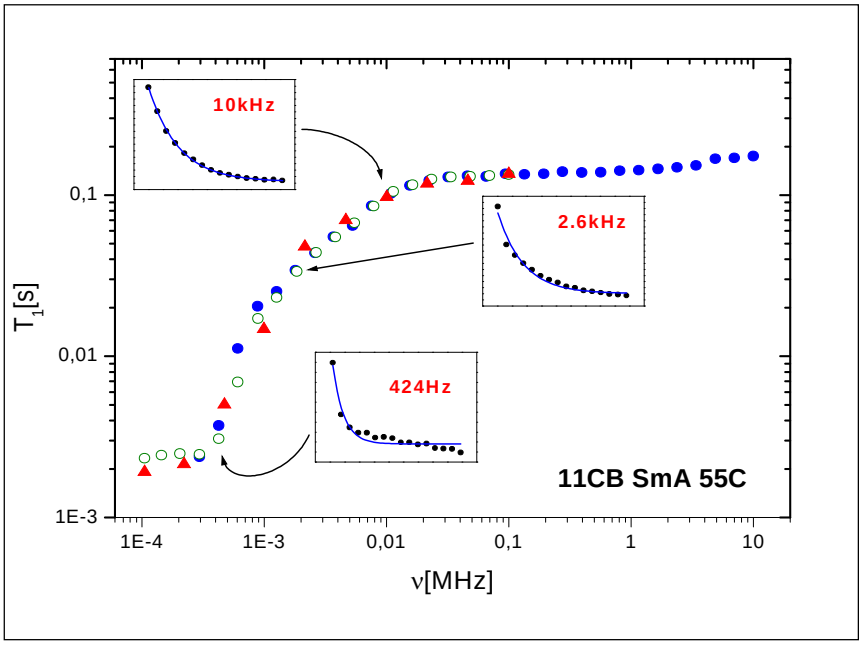

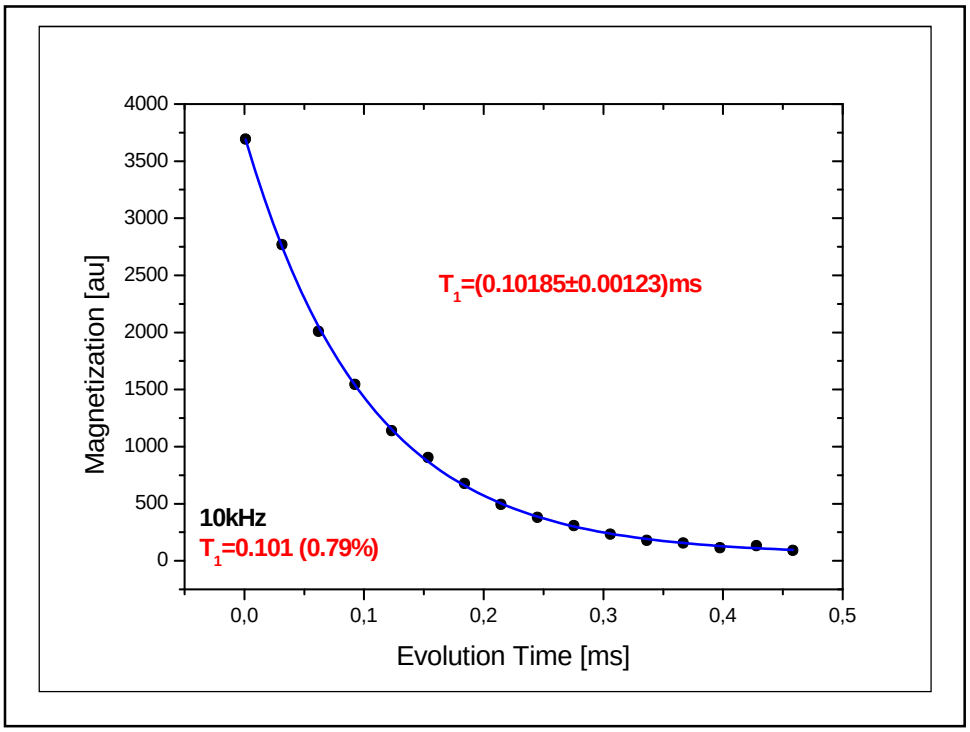
4000
3500
3000
2500
2000
1500
1000
500
0
Magnetization [au]
T1=(0.10185±0.00123)ms
10kHz
T1=0.101 (0.79%)
0,0
0,1
0,2
0,3
0,4
0,5
Evolution Time [ms]

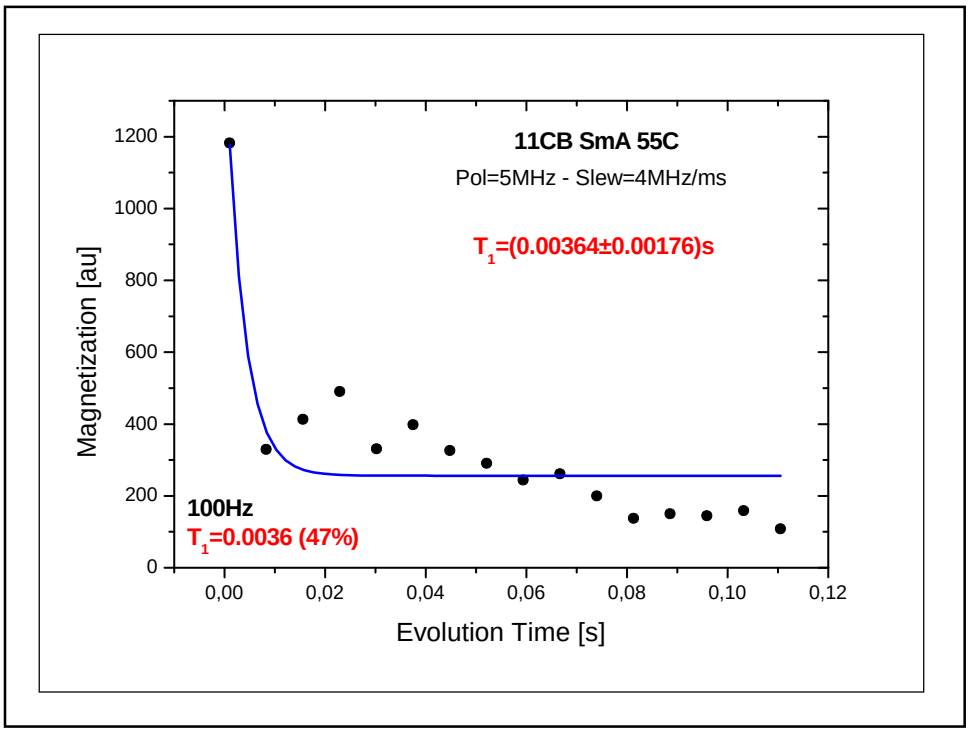
1200
1000
800
600
400
200
0
Magnetization [au]
11CB SmA 55C
Pol=5MHz - Slew=4MHz/ms
T1=(0.00364±0.00176)s
100Hz
T1=0.0036 (47%)
0,00
0,02
0,04
0,06
0,08
0,10
0,12
Evolution Time [s]

False dispersions

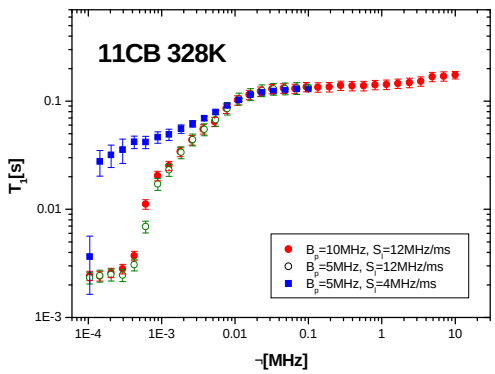

326K – 330,5K

Anoardo-Bonetto-Kimmich (2003)

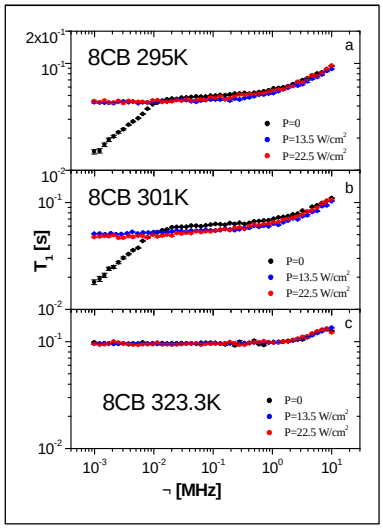

294,5K – 306,5K

Extreme conditions

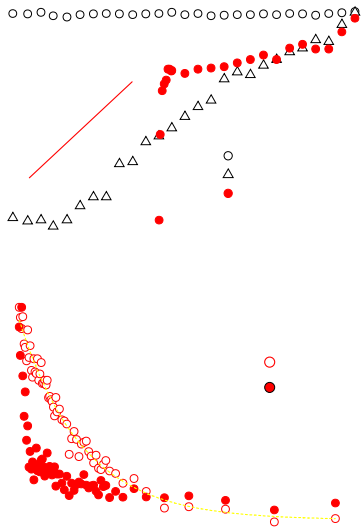

T_1 as an "order sensor"

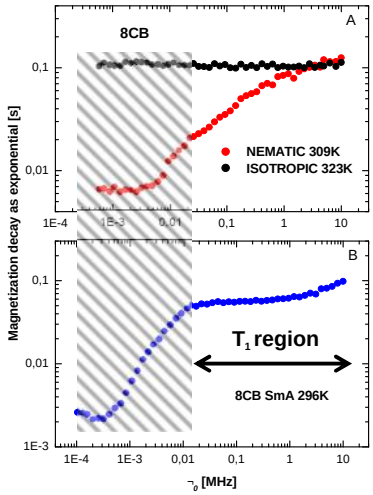

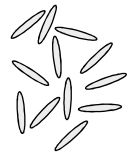

ISOTROPIC

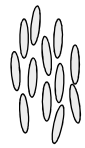

NEMATIC

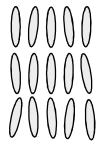

SMECTIC A

Fundamental point

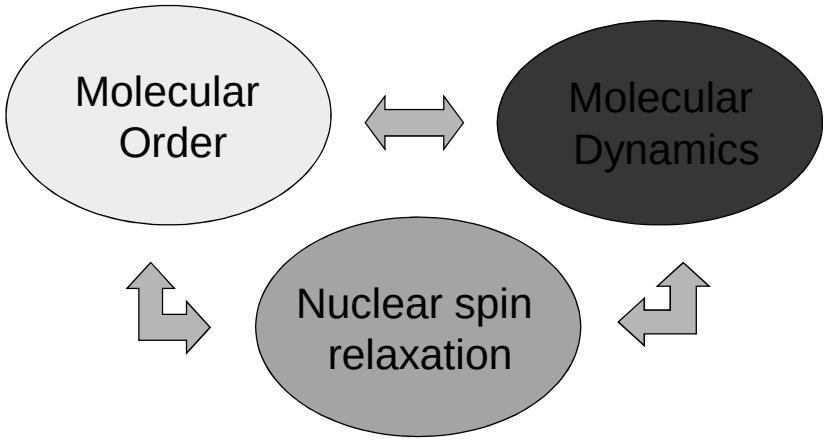

The action of sound on a nematic

VOLUME 29, NUMBER 24 PHYSICAL REVIEW LETTERS 11 DECEMBER 1972

Orienting Action of Sound on Nematic Liquid Crystals

W. Helfrich
Physics Department, F. Hoffmann-La Roche & Co., Basle, Switzerland
(Received 5 July 1972)

The orienting action of ultrasound on liquid crystals related to the theorem of minimum entropy production[a)]

Jean-Luc Dion
Département d'Ingénierie, Université du Québec à Trois-Rivières, Québec, G9A 5H7, Canada
(Received 22 August 1978; accepted for publication 10 October 1978)

ELSEVIER
30 July 2002
Chemical Physics Letters 361 (2002) 237–244
CHEMICAL PHYSICS LETTERS
www.elsevier.com/locate/cplett

Enhancement of order fluctuations in a nematic liquid crystal by sonication

F. Bonetto [a,1], E. Anoardo [a,*,2], R. Kimmich [b]
[a] *Facultad de Matemática, Astronomía y Física, Universidad Nacional de Córdoba, Ciudad Universitaria, C.P. 5000 Córdoba, Argentina*
[b] *Sektion Kernresonanzspektroskopie, Universität Ulm, 89069, Ulm, Germany*
Received 7 November 2001; in final form 8 May 2002

A second model is proposed on the basis that ultrasonic waves may change the molecular orientation [18,19]. Within this frame, a new term of the form $\frac{1}{2}Q_{SL}(\hat{n}\cdot\hat{q}_a)^2$ is proposed for the free energy density. In this expression, Q_{SL} is a constant independent of the wave vector $\vec{q}$ and

30 years later..

$$\langle V_{int}\rangle = \frac{u_2\rho_0 I}{v^3}(\mathbf{k}\cdot\hat{\mathbf{n}})^2.$$

PHYSICAL REVIEW E 66, 051708 (2002)

Acoustic realignment of nematic liquid crystals

J. V. Selinger, M. S. Spector, V. A. Greanya, B. T. Weslowski, D. K. Shenoy, and R. Shashidhar
Center for Bio/Molecular Science and Engineering, Naval Research Laboratory, Code 6900, 4555 Overlook Avenue SW, Washington, DC 20375
(Received 10 July 2002; published 19 November 2002)

Acoustic-Director fields interaction

$$\langle V_{\text{int}} \rangle = \frac{1}{2} Q(\mathbf{n}.\mathbf{q_a})^2$$

$$= \frac{1}{2} Q.q_a^2 \cos^2(\bar{\ } - \sim)$$

$$Q = \frac{2\P\,{}^{\circ}{}_{0} I}{v^3}$$

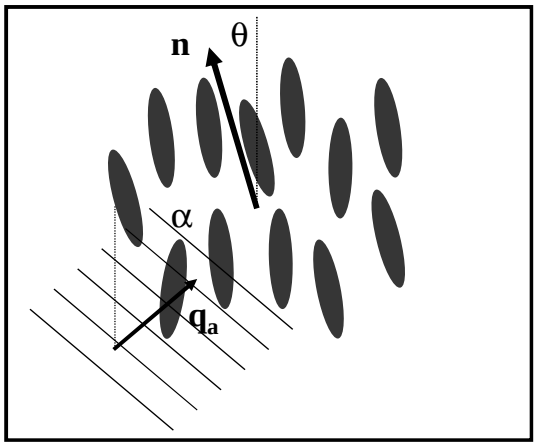

Bonetto-Anoardo-Kimmich (2002)

Selinger-Spector-Greanya-Weslowski-Shenoy-Shashidhar (2002)

Acoustic term: molecular reorientation

$$F_a = \frac{1}{2} Q(\mathbf{n}.\mathbf{q}_{\mathbf{a}})^2$$

$$F_m = -\frac{1}{2}\frac{\Delta \mathrm{i}}{«_0}(\mathbf{n}.\mathbf{B})^2$$

$$F = \frac{1}{2V}\sum_{\mathbf{q}}\sum_{\sim=1}^{2}\left|\mathbf{n}_{\sim}(\mathbf{q})\right|^2\left[Kq^2 - Q\right]$$

Experimental

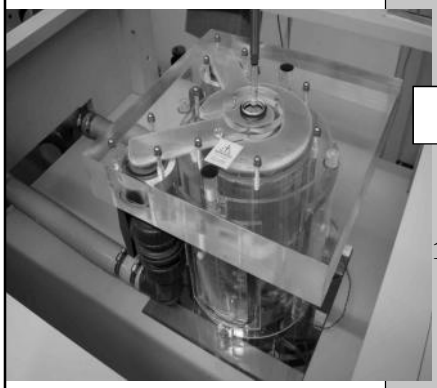

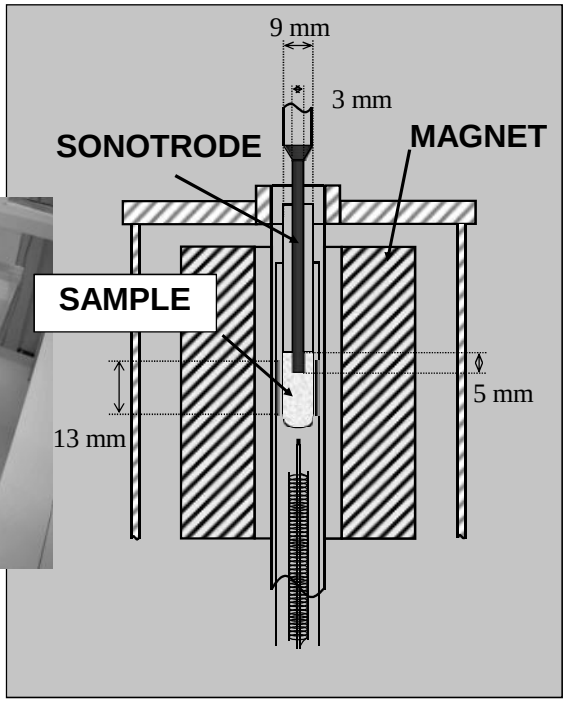

Effect of sonication in standard nematics

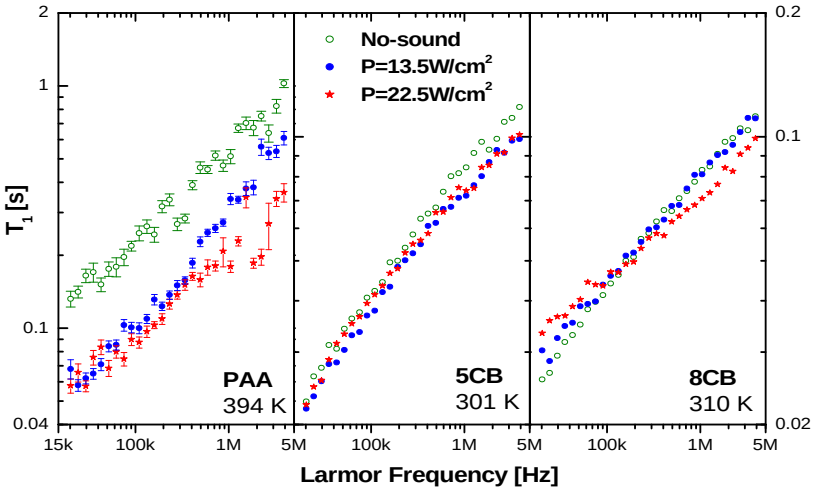

Bonetto-Anoardo-Kimmich (2003)

Magnetically ordered state

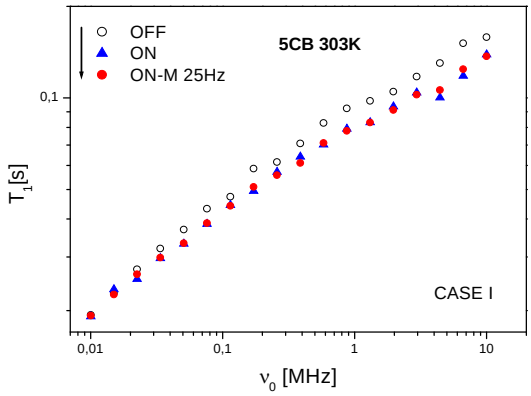

Acoustically ordered state

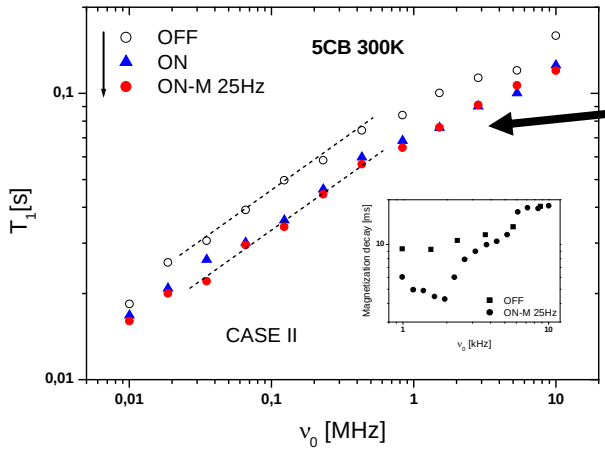

MEMORY OF ACOUSTIC ORDER

Comparison with angle-dependent field-cycling NMR relaxometry

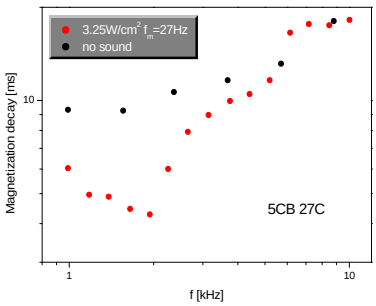

Struppe - Noack (1996)

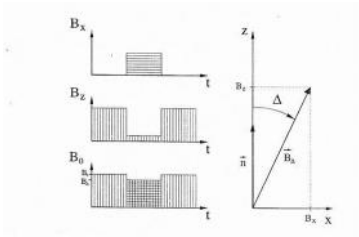

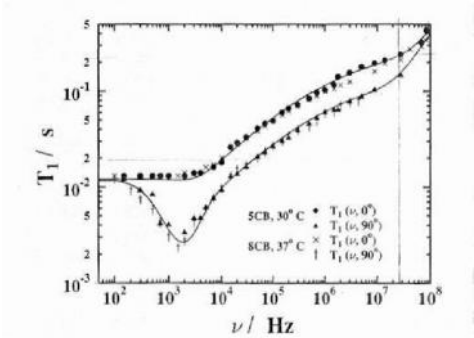

Relevant features

- Ultrasound mainly interacts with ODF
- **T_1 dispersion <u>is sensitive</u> to the interaction**
- Effects in the whole frequency window
- Efficient molecular reorientation

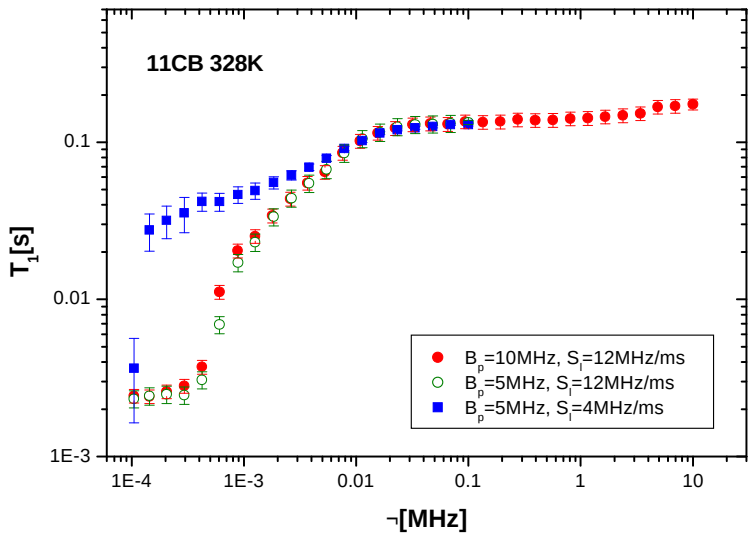

Sonication effect at low frequencies

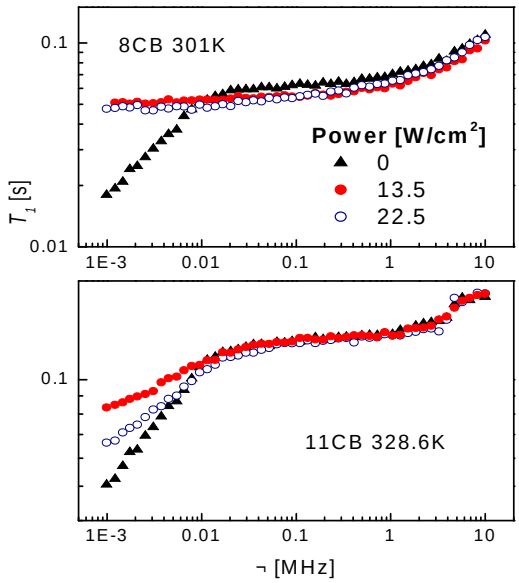

Anoardo – Bonetto – Kimmich (2003)

$\oint \hat{\mathbf{n}}\cdot d\mathbf{l} = 0.$ → This means that $\nabla\times\hat{\mathbf{n}} = 0$. Twist and bend elastic deformations do not occur in a perfect smectic A crystal. → $I_1^{\mathrm{ODF}}(\omega) = \dfrac{S^2 k_B T}{4K_{11}\xi_z}\omega^{-1},$

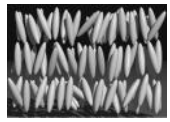

$$f_e = \frac{\beta}{2}\sigma_z^2 + \frac{1}{2}K_{11}(\nabla\cdot\hat{\mathbf{n}})^2. \qquad f_{Sm} = a(T)|\Psi|^2 + b(T)|\Psi|^4 + \cdots, \qquad f_{Sm-N} = (\nabla + iq_0\delta\hat{\mathbf{n}})\Psi^* \frac{1}{2M}(\nabla - iq_0\delta\hat{\mathbf{n}})\Psi,$$

$$f_{SmA} = f_e + f_{Sm} + f_{Sm-N}, \qquad \rho(\mathbf{r}) = \rho_0\left[1 + \frac{1}{2}|\Psi|\cos(q_0 z + \varphi)\right].$$

PHYSICAL REVIEW E **68**, 021703 (2003)

Spin-lattice dispersion in nematic and smectic-A mesophases in the presence of ultrasonic waves: A theoretical approach

F. Bonetto* and E. Anoardo†
Facultad de Matemática, Astronomía y Física, Universidad Nacional de Córdoba – Ciudad Universitaria, X5016LAE Córdoba, Argentina

$$j_{1,1}^{OF+S}(\omega) = \frac{3K_B T\eta_1}{4\sqrt{2}\pi\sqrt{D}K_{11}^{3/2}}\frac{B}{D}\int_0^1 \frac{dx}{\left[\frac{B}{D}(1-x^2)+\frac{K_{33}}{K_{11}}x^2\right]^{3/2}\sqrt{x^2-(+)\frac{a^2}{D}+\sqrt{\left(x^2-(+)\frac{a^2}{D}\right)^2+\left(\frac{\omega}{\omega_{z1}}\right)^2}}}.$$

$$f = f_n + f_z + f_I + f_a,$$

$$T_1^{OF+S}(\omega) = \beta[j_{1,1}^{OF+S}(\omega) + j_{1,2}^{OF+S}(\omega)]^{-1} = \beta\left\{\frac{3K_B T}{4\sqrt{2}\pi}\left[\frac{1}{\sqrt{D}}\eta_1 K_{11}^{-3/2}Y + \frac{4\sqrt{2}\pi}{3K_B T}j_{1,2}^{OF+S}(\omega)\right]\right\}^{-1}.$$

$$Y = \frac{B}{D}\int_0^1 \frac{dx}{\left(\frac{B}{D}(1-x^2)+\frac{K_{33}}{K_{11}}x^2\right)^{3/2}\sqrt{x^2-(+)\frac{a^2}{D}+\sqrt{\left(x^2-(+)\frac{a^2}{D}\right)^2+\left(\frac{\omega}{\omega_{z1}}\right)^2}}}.$$

It can be observed that in the absence of ultrasound waves ($a=0$), the calculated expression in Ref. [20] is reobtained (even though the expression obtained here in the absence of ultrasound seems to be different from the one obtained by Vilfan Kogof, and Blinc [20], it can be verified that they are the same). It is also important to notice that only one (ω_{z2})

Effects of sound in the smectic A phase

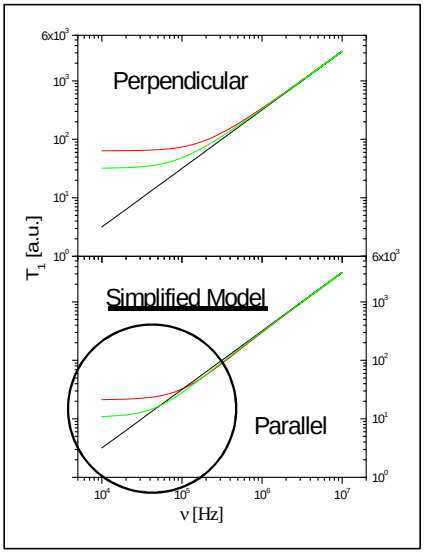

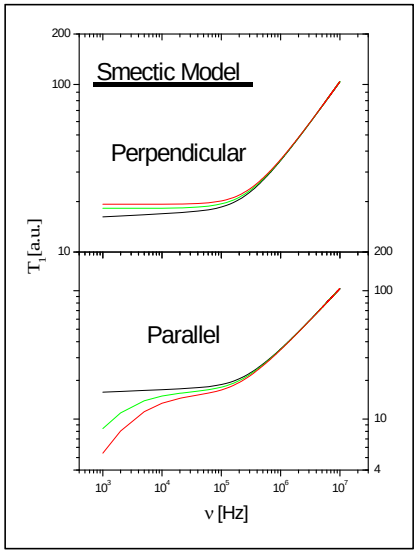

- **Smectic-model**
- **q_a \\ n**

The sound allows to display ODF

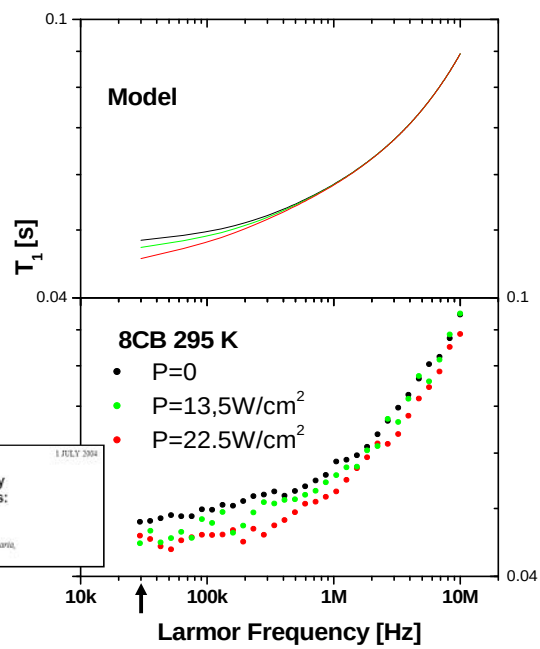

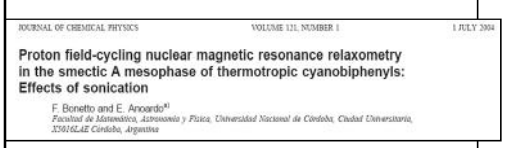
JOURNAL OF CHEMICAL PHYSICS VOLUME 121, NUMBER 1 1 JULY 2004

Proton field-cycling nuclear magnetic resonance relaxometry in the smectic A mesophase of thermotropic cyanobiphenyls: Effects of sonication

F. Bonetto and E. Anoardo[a]
Facultad de Matemática, Astronomía y Física, Universidad Nacional de Córdoba, Ciudad Universitaria, X5016LAE Córdoba, Argentina

V- Membranas lipídicas

Frequency dependence of NMR spin lattice relaxation in bilayer membranes

J. A. Marqusee
Department of Pharmaceutical Chemistry, School of Pharmacy, University of California, San Francisco, California 94143

Mark Warner
Rutherford and Appleton Laboratories, Chilton, Didcot, Oxfordshire, England OX11 0QX

Ken A. Dill
Department of Pharmaceutical Chemistry, School of Pharmacy, University of California, San Francisco, California 94143

6404 J. Chem. Phys. 81 (12), Pt. II, 15 Dec. 1984

$$J_{\text{dir}}(\omega_0) = S^2 \int_{-\infty}^{+\infty} dt\, e^{-i\omega_0 t} \langle \delta \mathbf{N}(\mathbf{r}, t) \cdot \delta \mathbf{N}(\mathbf{r}, 0) \rangle,$$

Recently it has been suggested that the NMR spin-lattice relaxation rates of nuclei in surfactant bilayer membranes should have the same frequency dependence as in nematic liquid crystals.[1–4] Bilayers are interfacial phases of matter, however, and thus have properties more characteristic of two-dimensional systems than of three-dimensional bulk phases such as nematics.[5] The purpose of this note is to show that these frequency dependences are different, but that they cannot be distinguished by the currently available experiments which cover a relatively narrow frequency range.

We have assumed that no coupling occurs between individual membranes in the same solution. This is undoubtedly justified for unilamellar vesicles. We expect that multilamel-

$$J_{\text{dir}}(\omega_0) = S^2 \frac{k_B T}{2K_c} \frac{1}{\omega_0} \left(\frac{1}{x}\right).$$

J. Phys. Chem. 1988, 92, 2981–2987

Proton Spin Relaxation Dispersion Studies of Phospholipid Membranes

Eberhard Rommel, Friedrich Noack,*

Physikalisches Institut, Universität Stuttgart, Pfaffenwaldring 57, D-7000 Stuttgart 80, West Germany

Peter Meier, and Gerd Kothe

Institut für Physikalische Chemie, Universität Stuttgart, Pfaffenwaldring 55, D-7000 Stuttgart 80, West Germany *(Received: November 3, 1987)*

This paper presents measurements of the proton spin T_1 relaxation dispersion of phospholipid membranes of 1,2-dimyristoyl-*sn*-glycero-3-phosphocholine (DMPC) over a very broad Larmor frequency range (100 Hz $\leq \omega/2\pi \leq$ 300 MHz). The results show that, in contrast to suggestions in the literature, collective molecular reorientations (order fluctuations) contribute to the proton relaxation process only at extremely low frequencies in the kilohertz regime, whereas the conventional high-frequency range is dominated by reorientation of individual molecules. The order fluctuations are observed by a characteristic $T_1(\omega) \sim \omega^1$ dispersion at low frequencies for both the liquid crystalline and intermediate phases of the model membranes, which is completely absent for the "crystalline" gel phase and for isotropic liquid phases of DMPC molecules.

DMPC: 1,2-Dimyristoyl-sn-glycero-3-phosphocholine- 1:1 in D_2O.
Multilamellar

The low-frequency relaxation dispersion in the liquid crystalline state shows a broad interval where $T_1(\omega)$ is proportional to ω^1.

Obviously, the rich experimental details, revealed by Figures 1 and 2, cannot be interpreted quantitatively by a relaxation model restricted to one single process, say by the $T_1(\omega) \sim \omega^{1/2}$ or $T_1(\omega) \sim \omega^1$ laws favored by Brown et al.[1-6] or Marqusee et al.[11] A

the two concepts. However, as an alternative to Kimmich's defect diffusion approach, we employed a less specific model for the individual molecular reorientations,[30-33] which avoids several assumptions not appropriate for the liquid crystalline phase.[34]

When we tried to fit such a superposition of two processes to our $T_1(\omega)$ and $T_1(T)$ measurements in a self-consistent way, it was easily recognized that a combination of only two relaxation mechanisms did not yield satisfactory results. In particular, the

Following these arguments we present a quantitative evaluation of the data of the liquid crystalline phase in terms of relaxation by smectic *o*rder *f*luctuations of groups of molecules (relaxation rate $1/T_1^{(OF)}$),[11,12] internal and overall *m*olecular *r*otations of individual molecules (relaxation rate $1/T^{(MR)}$),[30–33] *l*ateral *d*iffusion of molecules in the bilayer plane (relaxation rate $1/T_1^{(LD)}$),[44–46] and *t*ranslationally induced *r*otations of molecules on curved bilayer regions (relaxation rate $1/T_1^{(TR)}$).[47] This model implies a cor-

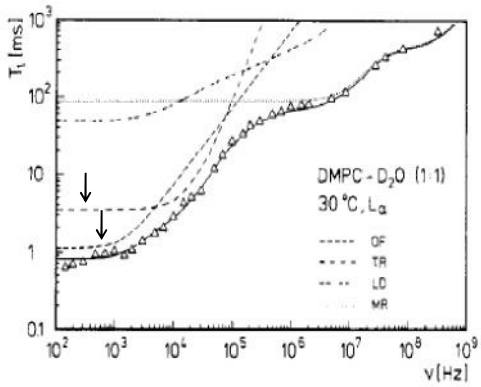

- **Order fluctuations (smectic)**
- **Translationally induced rotations (diffusion on curved surfce)**
- **3 rotational terms (Lorentzian)**
- **Lateral diffusion (Vilfan's for smectic)**

NMR Study of Collective Motions and Bending Rigidity in Multilamellar System of Lipid and Surfactant Bilayers

J. Struppe[a], F. Noack[a], and G. Klose[b]

[a] Universität Stuttgart, Physikalisches Institut Teil 4, Pfaffenwaldring 57, D-70550 Stuttgart
[b] Universität Leipzig, Physikalisches Institut Abteilung BIM, Linnéstr. 5, D-04103 Leipzig

Z. Naturforsch. **52a**, 681–694 (1997); received March 29, 1997

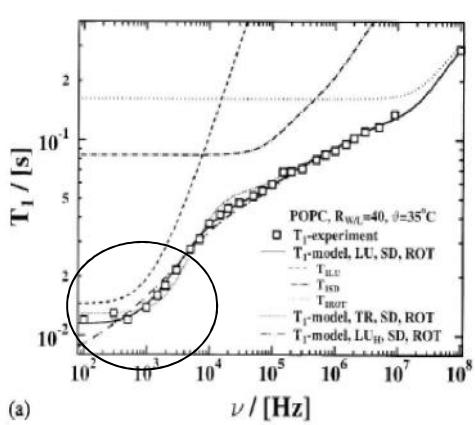

- **Compares coupled/uncoupled layers**
- **OF physical parameters inconsistent respect other experimental techniques**
- **Discussion focused in the low-frequency end of the dispersion (cut-off's).**

Features

- Interpretations based on available theoretical models
- Too many fitting parameters

Alternatives

- Model-free approach
- Evidence-based interpretation. Fixed parameters from other experiments. Model refinement when needed.

~~Fitting~~ → **Simulation**

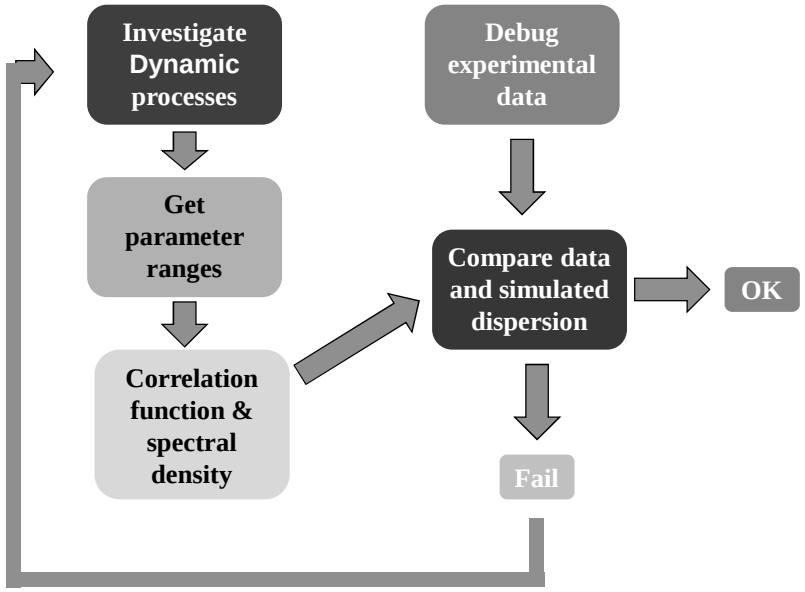

Physica A 163 (1990) 410–428
North-Holland

BENDING ELASTICITY AND THERMAL EXCITATIONS OF LIPID BILAYER VESICLES: MODULATION BY SOLUTES

H.P. DUWE and E. SACKMANN
Physics Department, Biophysics Group, Technische Universität München, D-8046 Garching, Fed. Rep. Germany

$$r(\vartheta, \varphi, t) = r_0\left(1 + \sum_{l,m}^{\infty} a_{l,m}(t) Y_{l,m}(\vartheta, \varphi)\right),$$

The thermal excitations of quasi-spherical vesicles are described in terms of a spherical harmonics expansion ($Y_{lm}(\vartheta, \varphi)$) of the middle surface separating the two monolayers. The latter is determined by the radius $r(\vartheta, \varphi)$ (ϑ: polar angle,

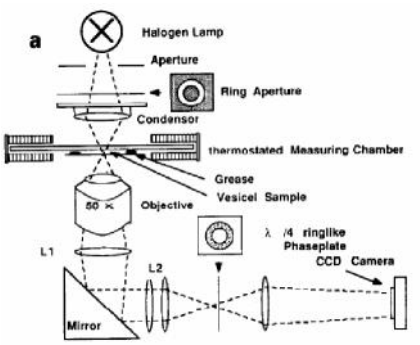

Eur Biophys J (2004) 33: 732–741
DOI 10.1007/s00249-004-0420-5

ARTICLE

Jonas Henriksen · Amy C. Rowat · John H. Ipsen

Vesicle fluctuation analysis of the effects of sterols on membrane bending rigidity

The vesicles undergo undulations in shape which can be observed using light microscopy and subsequently

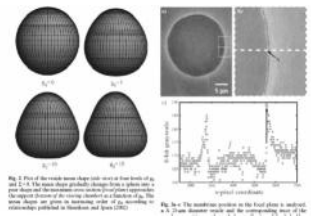

PHYSICAL REVIEW E 71, 021905 (2005)

Viscoelastic dynamics of spherical composite vesicles

S. B. Rochal,[1,2] V. L. Lorman,[1] and G. Mennessier[1]
[1]*Laboratoire de Physique Mathematique et Théorique, CNRS-Université Montpellier 2, Place Eugène Bataillon, 34095 Montpellier, France*
[2]*Physical Faculty, Rostov State University, 5 Zorge Street, 344090 Rostov-on-Don, Russia*
(Received 6 October 2003; revised manuscript received 21 October 2004; published 11 February 2005)

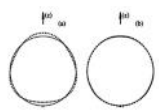

$$\mathbf{u}_\perp = \sum_{l=0}^{l=\infty} \sum_{m=-l}^{m=l} A_{lm}^{Y} Y_{lm}(\theta, \phi)\mathbf{e}_r.$$

PHYSICAL REVIEW E, VOLUME 64, 022902

Nuclear-spin relaxation induced by shape fluctuations in membrane vesicles

M. Vilfan,[1] G. Althoff,[2] I. Vilfan,[1] and G. Kothe[2]
[1]*J. Stefan Institute, Jamova 39, SI-1000 Ljubljana, Slovenia*
[2]*Department of Physical Chemistry, University of Freiburg, Albertstrasse 21, D-79104 Freiburg, Germany*
(Received 31 March 2001; published 26 July 2001)

Nuclear-spin relaxation rates resulting from shape fluctuations of *multilamellar quasispherical vesicles* are calculated. We show that in the kHz range these fluctuations yield—in contrast to previous conclusions on planar membranes – a relaxation rate proportional to the inverse Larmor frequency and provide direct information on the bending rigidity of membranes.

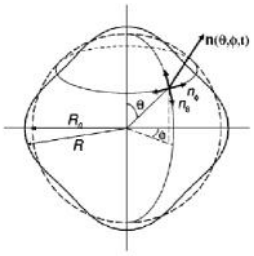

$$R(\theta, \phi) = R_0[1 + u(\theta, \phi)],$$

$$u(\theta, \phi) = \sum_{l} \sum_{m=-l}^{l} u_{l,m} Y_{l,m}(\theta, \phi).$$

$$J(\omega) = \frac{k_B T}{4\pi\kappa} \sum_{l=2}^{l_{\max}} \frac{l(l+1)(2l+1)}{(l^2+l-2)(l^2+l+\sigma)} \frac{2\tau_l}{(1+\omega^2\tau_l^2)}. \quad (10)$$

$$J(\omega) = \mathrm{Re} \int_{-\infty}^{+\infty} [\langle n_\theta(0) n_\theta^*(t)\rangle + \langle n_\phi(0) n_\phi^*(t)\rangle] e^{-i\omega t} dt.$$

$$n_\theta = -\frac{\partial u(\theta, \phi)}{\partial \theta}, \quad n_\phi = -\frac{1}{\sin\theta} \frac{\partial u(\theta, \phi)}{\partial \phi}.$$

$$\tau_l = \frac{\eta R_0^3}{\kappa} \frac{(2l+1)(2l^2+2l-1)}{l(l+1)(l+2)(l-1)(l^2+l+\sigma)}.$$

3758 Biophysical Journal Volume 85 December 2003 3758–3768

Lipid Dynamics and Domain Formation in Model Membranes Composed of Ternary Mixtures of Unsaturated and Saturated Phosphatidylcholines and Cholesterol

Dag Scherfeld,* Nicoletta Kahya,*† and Petra Schwille†
*Experimental Biophysics Group, Max Planck Institute for Biophysical Chemistry, Göttingen, Germany; and †Dresden University of Technology, c/o Max Planck Institute of Molecular Cell Biology and Genetics, Dresden, Germany

fast fluorescence recovery in a bleached spot. recovery after photobleaching of a squared spot. Fluorescence recovery did not occur within hours. GUVs made

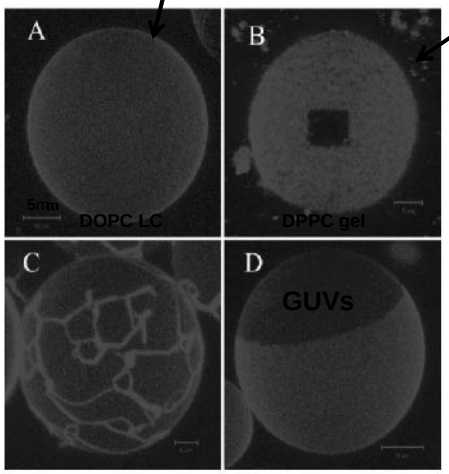

Confocal fluorescence microscopy

FRAP Axelrod, D., Koppel, D.E., Schlessinger, J., Elson, E., Webb, W.W., 1976. Mobility measurements by analysis of fluorescence photobleaching recovery kinetics. Biophys. J. 16, 1055–1069.

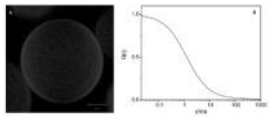

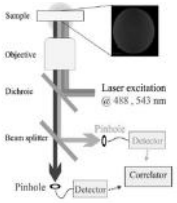

FCS

$$G(\tau) = \frac{\langle \delta F(t+\tau)\delta F(t)\rangle}{\langle F(t)\rangle^2} = \frac{\langle \delta F(\tau)\delta F(0)\rangle}{\langle F\rangle^2}.$$

$$G(\tau) = \frac{\left(\sum_i \langle C_i\rangle \left(\frac{1}{1+\tau/\tau_{d,i}}\right)\right)}{A_{\mathrm{eff}}\left(\sum_i \langle C_i\rangle\right)^2}.$$

D~7E-12m²/s

$$\tau_{d,i} = r_0^2/4D_i.$$

i: chemical specimen

Theory of spin relaxation by diffusion on curved surfaces

Bertil Halle
Physical Chemistry 1, University of Lund, Chemical Center, P. O. Box 124, S-22100 Lund, Sweden

$$p = \frac{1}{r} = \frac{a}{b},$$

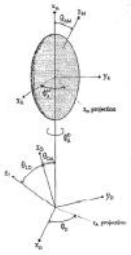

B. Isotropic micellar solutions

In isotropic systems, where the tensorial spin-lattice coupling is isotropically averaged by sufficiently fast motions, there is only one lab-frame spectral density function. According to (3.6)

$$j^{\mu}(\omega) = \frac{1}{5} S^2_{\Lambda M} \frac{\tau_0}{1+(\omega\tau_0)^2} + \frac{1}{5}\sum_{m=-2}^{2}(2-\delta_{m0}) \times \int_0^{\infty} dt \cos(\omega t)\exp(-t/\tau_m) g^{\Lambda M}_{m}(t), \quad (7.3)$$

where the symmetric top correlation times τ_m are related to the rotational diffusion coefficients $D_\parallel$ and $D_\perp$ through (3.5).

In the sphere limit, (3.5) and (5.14) show that (7.3) reduces to the Lorentzian

$$j^{\mu}(\omega) = \frac{1}{5}\frac{\tau_R}{1+(\omega\tau_R)^2}, \quad (7.4)$$

with the joint correlation time τ_R being related to the rotational-diffusion correlation time τ_{rd} and the surface-diffusion correlation time τ_{sd} by

$$\frac{1}{\tau_R} = \frac{1}{\tau_{rd}} + \frac{1}{\tau_{sd}}, \quad (7.5)$$

$$\tau_{rd} = \frac{1}{6D_r} = \frac{4\pi\eta b^3}{3k_B T}, \quad (7.6)$$

$$\tau_{sd} = \frac{b^2}{6D_s}, \quad (7.7)$$

frequency spectral density $j^{\mu}(0)$.] Figure 7 shows that the departure from a Lorentzian dispersion can be substantial already at $p = 1.3$. For a prolate micelle, this corresponds to an increase in the aggregation number by 30%. While changes in aggregation number of this order of magnitude can probably be determined by other techniques, such as fluorescence quenching[41] and neutron scattering,[42] nuclear spin relaxation appears to be a unique method for revealing small deviations from spherical shape.

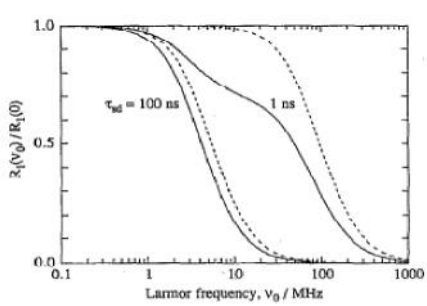

FIG. 7. Normalized frequency dispersion of isotropic longitudinal relaxation rate due to surface diffusion on freely rotating spheres (dashed curves) and prolate spheroids of axial ratio $p = 1.3$ (solid curves). The rotational correlation time is $\tau_{rd} = 20$ ns.

3150 J. Chem. Phys. 94 (4), 15 February 1991

Fast motions

- Thermally activated processes

- vibrational fluctuations
- librations
- isomerizations
- fast rotational processes
- hydrocarbon chains fluctuations
- etc……

In the explored time scale: manifested as a frequency independent offset

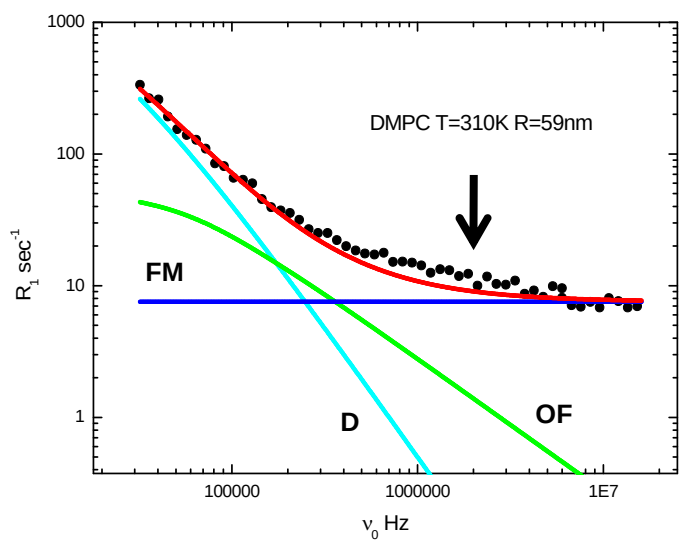

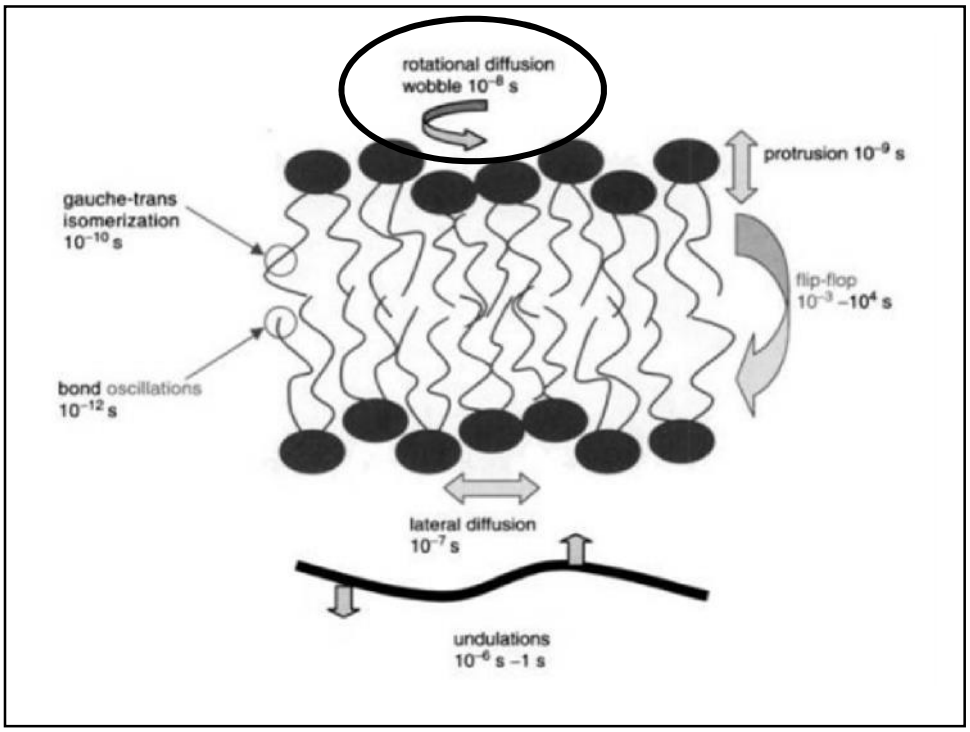

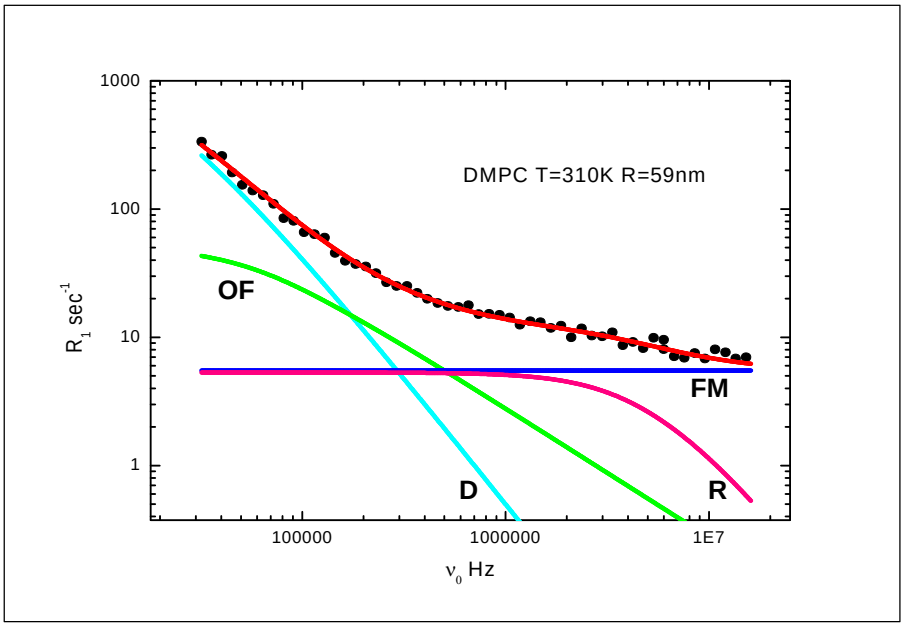

Meledandri, Perlo, Farrher, Brogham, Anoardo (2009)

Similar result for DOPC

15532 J. Phys. Chem. B 2009, 113, 15532–15540

Interpretation of Molecular Dynamics on Different Time Scales in Unilamellar Vesicles Using Field-Cycling NMR Relaxometry

Carla J. Meledandri,[†] Josefina Perlo,[‡] Ezequiel Farrher,[‡] Dermot F. Brougham,[*,†] and Esteban Anoardo[*,‡]

National Institute for Cellular Biotechnology, School of Chemical Sciences, Dublin City University, Dublin 9, Ireland, and Larte - Famaf. Universidad Nacional de Córdoba and Instituto de Física Enrique Gaviola (CONICET), Córdoba, Argentina

THE JOURNAL OF PHYSICAL CHEMISTRY B ARTICLE

dx.doi.org/10.1021/jp2009034 | J. Phys. Chem. B 2011, 115, 3444–3451 pubs.acs.org/JPCB

Temperature and Size-Dependence of Membrane Molecular Dynamics in Unilamellar Vesicles by Fast Field-Cycling NMR Relaxometry

Josefina Perlo,[†,∥] Carla J. Meledandri,[‡,§,∥] Esteban Anoardo,[*,†] and Dermot F. Brougham[*,‡]

[†]Laboratorio de Relaxometría y Técnicas Especiales, Grupo de Resonancia Magnética Nuclear, Facultad de Matemática, Astronomía y Física, Universidad Nacional de Córdoba and IFEG (CONICET), Córdoba, Argentina

[‡]National Institute for Cellular Biotechnology, School of Chemical Sciences, Dublin City University, Dublin 9, Ireland

[§]Department of Chemistry, University of Otago, Dunedin, New Zealand

LaRTE

Cómo influye la dinámica de los lípidos la presencia de colestrol?

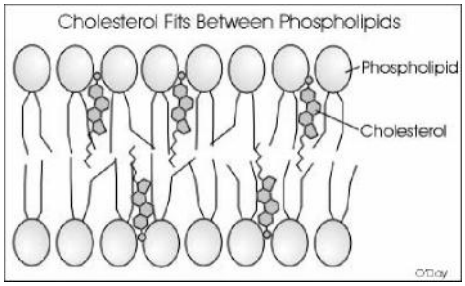

Microscopic approach (two lipid populations)

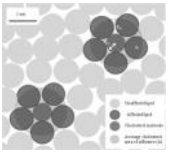

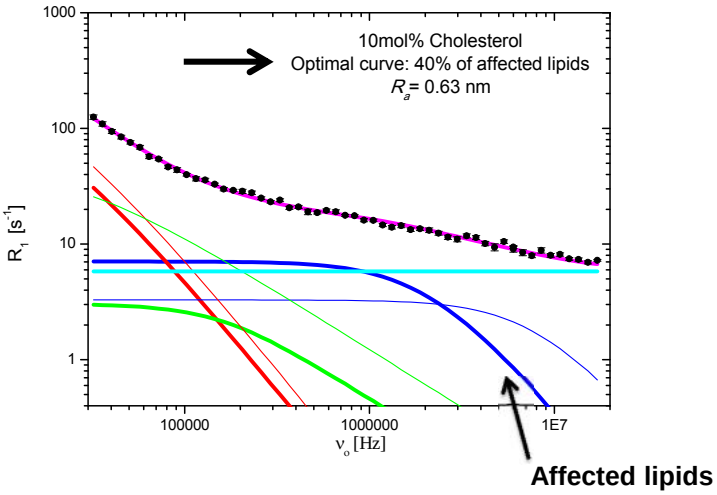

Microscopic approach

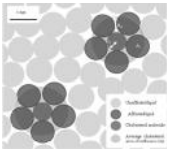

DOPC/10%
80nm 298K

40%
Affected lipids

Parameter	model value	
	Unaffected lipids (l_d phase)	Affected lipids (l_o phase)
η D_2O [Kg/s.m]	1.1×10^{-3}	1.1×10^{-3}
σ	0	0
a [nm]	1	1
Cholesterol area [nm^2]	----------	0.35
Lipid area [nm^2]	0.73	0.71
K [J]	$(5.4\pm0.8) \times 10^{-20}$	$(30\pm10) \times 10^{-20}$
A_{OF} [s^{-2}]	$(1.0\pm0.3) \times 10^{9}$	$(3\pm2) \times 10^{9}$
D [m^2/s]	$(1.3\pm0.4) \times 10^{-11}$	$(0.5\pm0.2) \times 10^{-11}$
τ_D [s]	$(0.7\pm0.2) \times 10^{-4}$	$(1.5\pm0.5) \times 10^{-4}$
A_D [s^{-2}]	$(1.0\pm0.3) \times 10^{9}$	$(2.1\pm0.9) \times 10^{9}$
τ_R [s]	$(1.1\pm0.3) \times 10^{-8}$	$(4.4\pm0.9) \times 10^{-8}$
A_R [s^{-2}]	$(1.0\pm0.3) \times 10^{8}$	$(0.8\pm0.1) \times 10^{8}$
$A_{FM} J_{FM}$ [s^{-1}]	(5.8 ± 0.6)	
R_a [nm]	----------	0.63
N° of affected lipids by cholesterol	----------	3.6

Microscopic approach

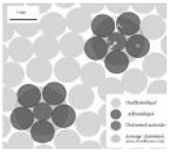

DOPC/25%
68nm 298K

90%

Affected lipids

Parameter	model value	
	Unaffected lipids (l_d phase)	Affected lipids (l_o phase)
η D_2O [Kg/s.m]	1.1×10^{-3}	1.1×10^{-3}
σ	0	0
a [nm]	1	1
Cholesterol area [nm^2]	----------	0.35
Lipid area [nm^2]	0.73	0.64
K [J]	$(5.4\pm0.9) \times 10^{-20}$	30×10^{-20}
A_{OF} [s^{-2}]	$(1\pm0.3) \times 10^{9}$	5.1×10^{9}
D [m^2/s]	$(8.8\pm0.3) \times 10^{-12}$	5.5×10^{-12}
τ_D [s]	$(0.7\pm0.2) \times 10^{-4}$	1×10^{-4}
A_D [s^{-2}]	$(1.3\pm0.2) \times 10^{9}$	4.3×10^{9}
τ_R [s]	$(1.1\pm0.3) \times 10^{-8}$	3.7×10^{-8}
A_R[s^{-2}]	$(2.0\pm0.3) \times 10^{8}$	0.9×10^{8}
$A_{FM} J_{FM}$ [s^{-1}]	8.4	
R_a [nm]	----------	0.48
N° of affected lipids by cholesterol	----------	2.7

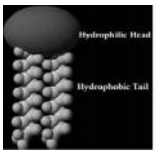

per

FFC → 3

Edholm (1992) → >3

Chiu (2002) → 8-9

Jedlovsky (2003) → 9

Alwarawrah (2010) → Supports Edholm

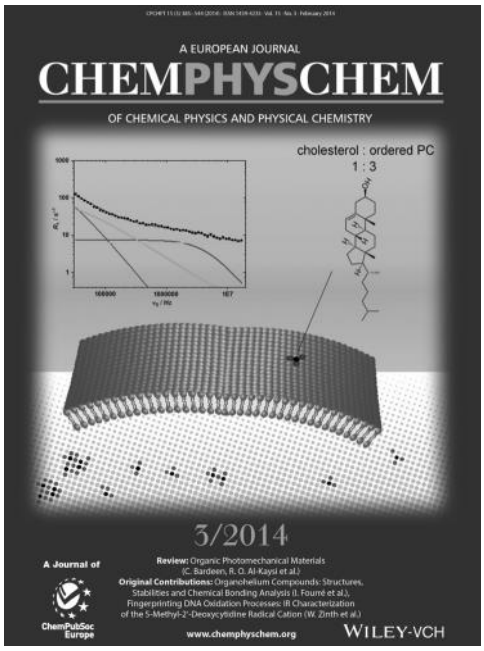
A EUROPEAN JOURNAL
CHEMPHYSCHEM
OF CHEMICAL PHYSICS AND PHYSICAL CHEMISTRY
cholesterol : ordered PC
1 : 3
3/2014
A Journal of
ChemPubSoc Europe
Review: Organic Photomechanical Materials (C. Bardeen, R. O. Al-Kaysi et al.)
Original Contributions: Organohelium Compounds: Structures, Stabilities and Chemical Bonding Analysis (I. Fourré et al.), Fingerprinting DNA Oxidation Processes: IR Characterization of the 5-Methyl-2'-Deoxycytidine Radical Cation (W. Zinth et al.)
www.chemphyschem.org
WILEY-VCH

Different approaches

- High detection field
- Superconducting magnet
- Keep spectroscopic resolution
- Typical switching times 50ms – 500ms
- Movable sample
- Pneumatic or mechanic system

- Moderate detection field
- Air-cored electromagnet
- Low resolution, relaxation applications
- Typical switching times 0.2ms – 2ms.
- Sample at fixed position
- Power electronics

Fast-Field-Cycling (FFC)

Block-diagram

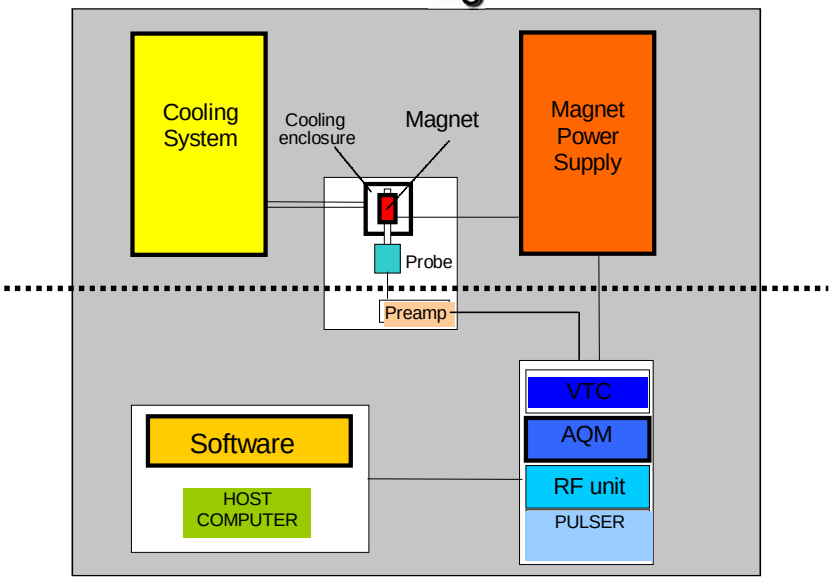

I- Power network

Basic circuit

$R_{high} \ll R_{low}$ and $R \ll R_{low}$

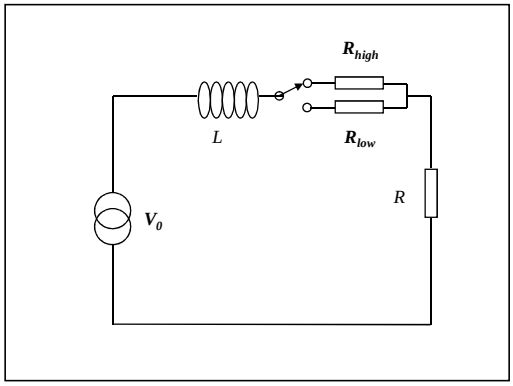

Low-to-high

Capacitor assistance

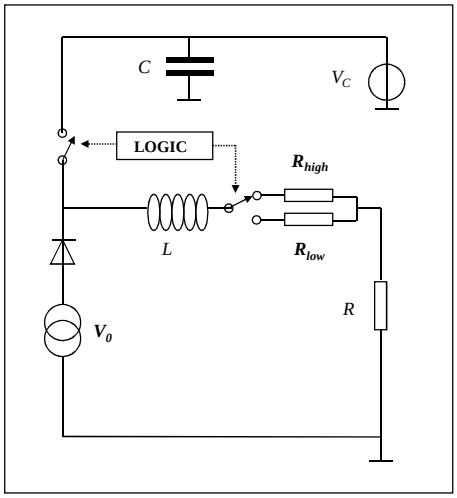

Vc » Vo

Examples

Mosfet – GTO. Energy-storage.

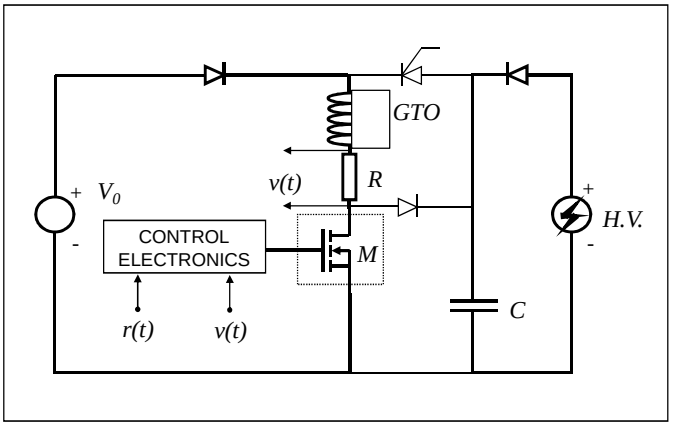

Mosfet-driven network without energy storage capacitor

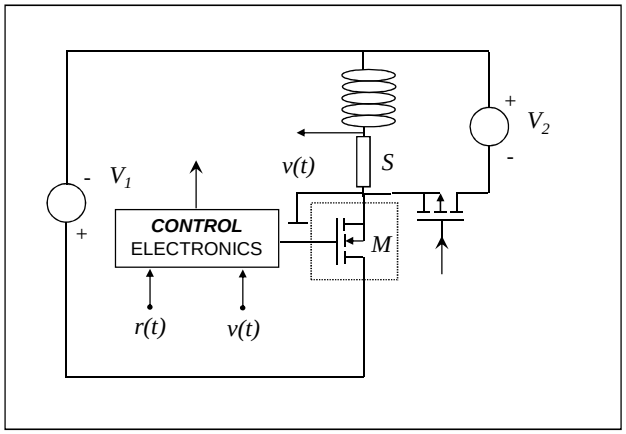

II- Magnet

Premises of design

- Low inductance and resistance.
- Good magnetic field to power ratio (G-factor).
- NMR homogeneity.
- Efficient cooling.
- Simple mechanical assembly.

Field-cycling magnets

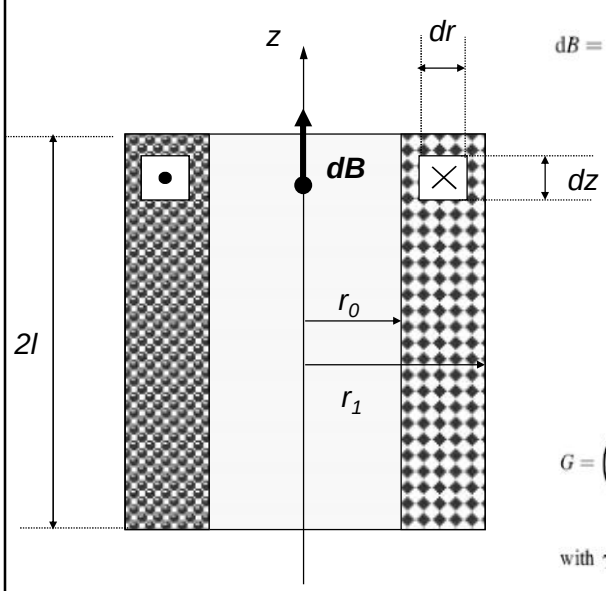

$$\mathrm{d}B = \left(\frac{\mu_0}{4\pi}\right)\xi_I f(r,z)\left[\frac{r^2}{(r^2+z^2)^{3/2}}\right]\mathrm{d}r\,\mathrm{d}z.$$

$$\mathrm{d}W = \left(\frac{\rho}{\lambda}\right)\xi_I^2 f^2(r,z)\,r\,\mathrm{d}r\,\mathrm{d}z,$$

$$B = G\sqrt{\frac{W\lambda}{\rho r_0}},$$

$$G = \left(\frac{\mu_0}{4\pi}\right)\frac{\int_{-\beta}^{+\beta}\mathrm{d}\gamma\int_1^{\alpha} f(\delta,\gamma)\frac{\delta^2\,\mathrm{d}\delta}{(\delta^2+\gamma^2)^{3/2}}}{\left[\int_{-\beta}^{+\beta}\mathrm{d}\gamma\int_1^{\alpha}\mathrm{d}\delta\, f^2(\delta,\gamma)\delta\right]^{1/2}}$$

with $\gamma = z/r_0$, $\delta = r/r_0$, $\alpha = r_1/r_0$ and $\beta = l/r_0$.

The Dvinskikh-Molchanov approach (1985)

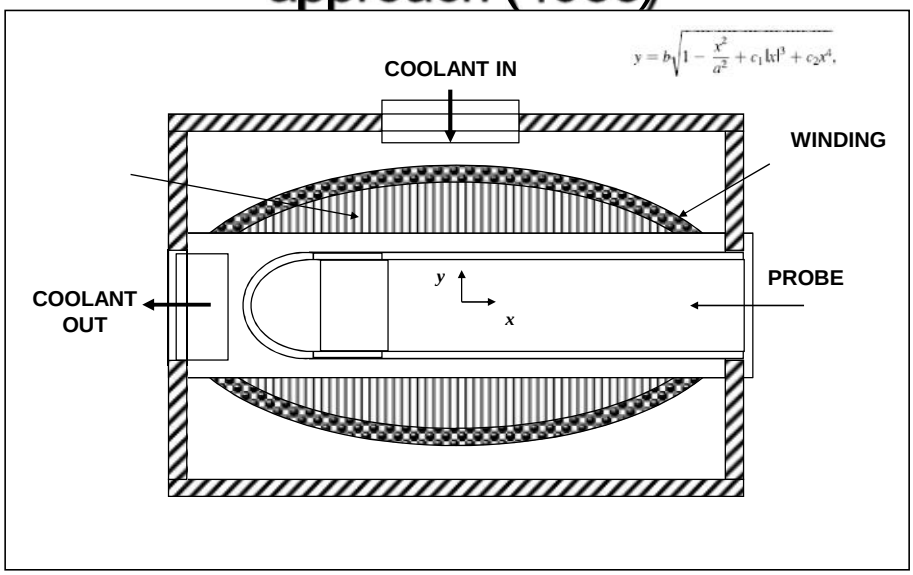

Schweikert-Noack Magnet (1989)

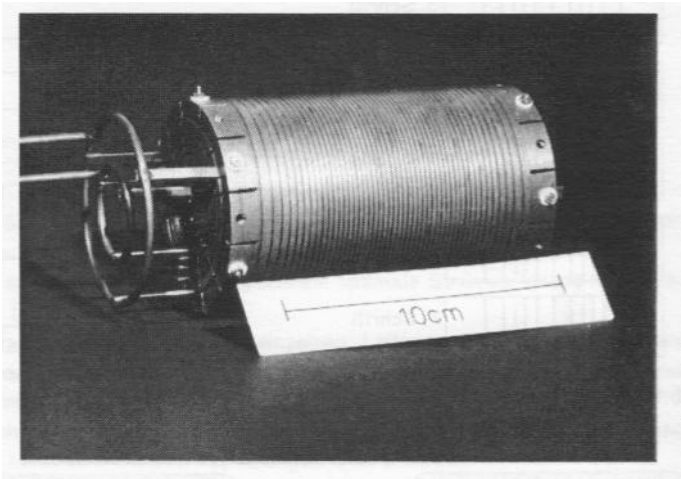

- Inversion of the Biot-Savart law

- Lagrange minimization procedure:
  field to power ratio, homogeneity and volume

Notch-coil

Rommel - Seitter - Kimmich

(1993-1995)

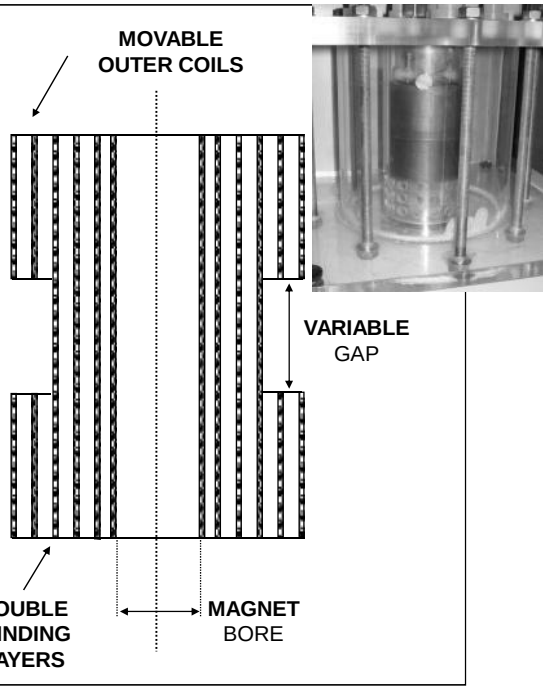

Stelar 2L-0.5T system (1997-2000)

Helical Notch (Larte – 2014)

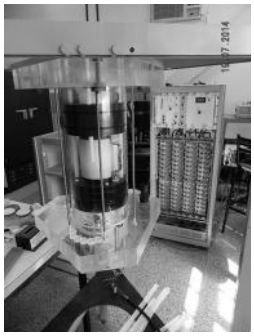

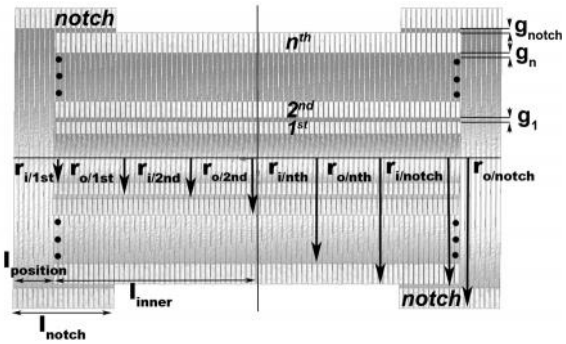

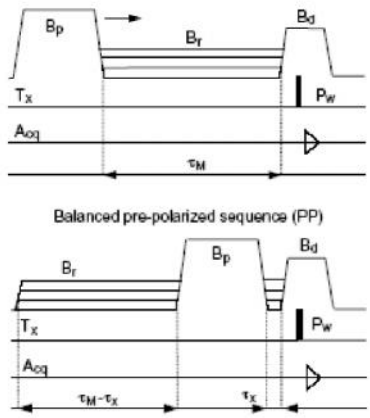

Fig. 18. Balanced multiblock pre-polarized sequence. The aim of the sequence is to keep constant the power dissipation at the magnet independently of the relaxation interval. The figure depicts the sequence for both the maximum evolution time τ_M (top) and for the minimum value of $\tau(\tau_X)$.

ULF regime

- External magnetic field components: magnetic field compensation.
- Internal magnetic field components: local fields.

Switching the Zeeman Field

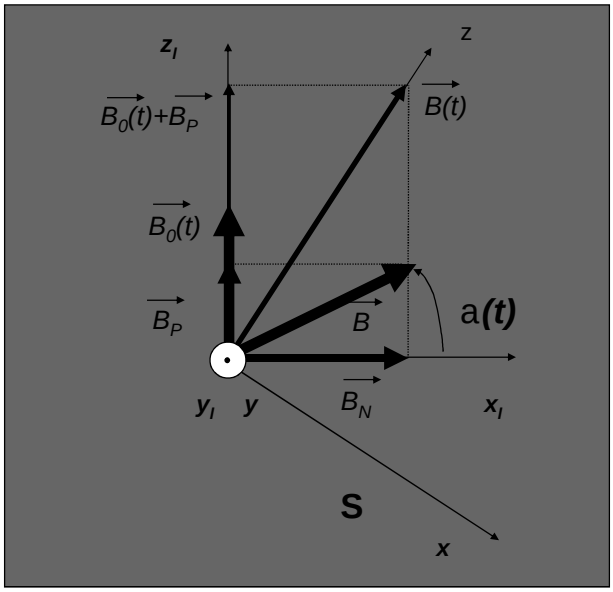

$$\frac{1}{B^2}\left|\vec{B}\times\frac{\mathrm{d}\vec{B}}{\mathrm{d}t}\right| \ll \gamma B,$$

Time-dependence of the field

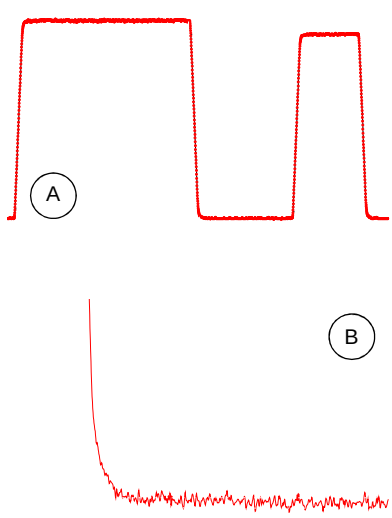

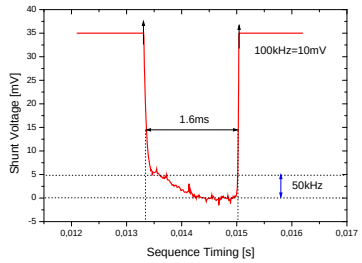

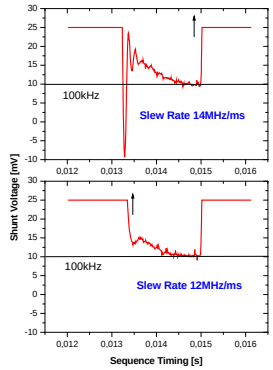

Adiabatic & non-adiabatic switching

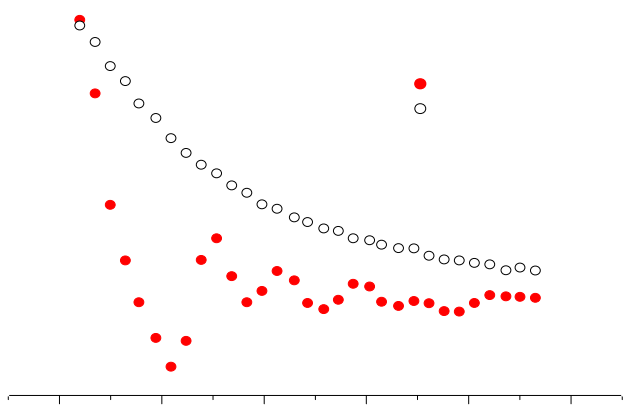

Magnetic field compensation

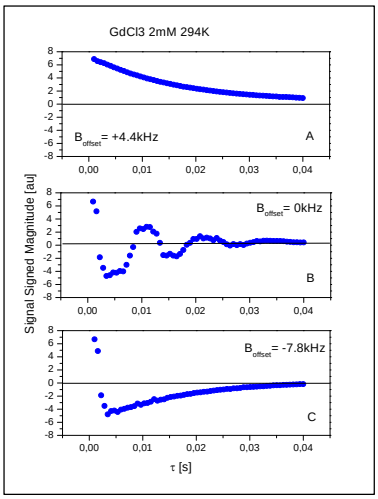

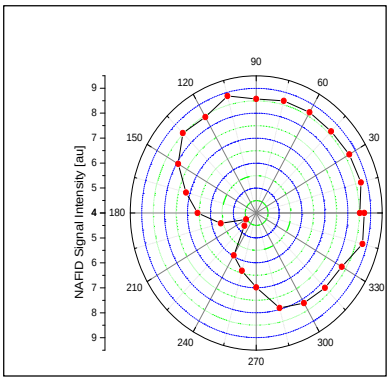

Figure 3

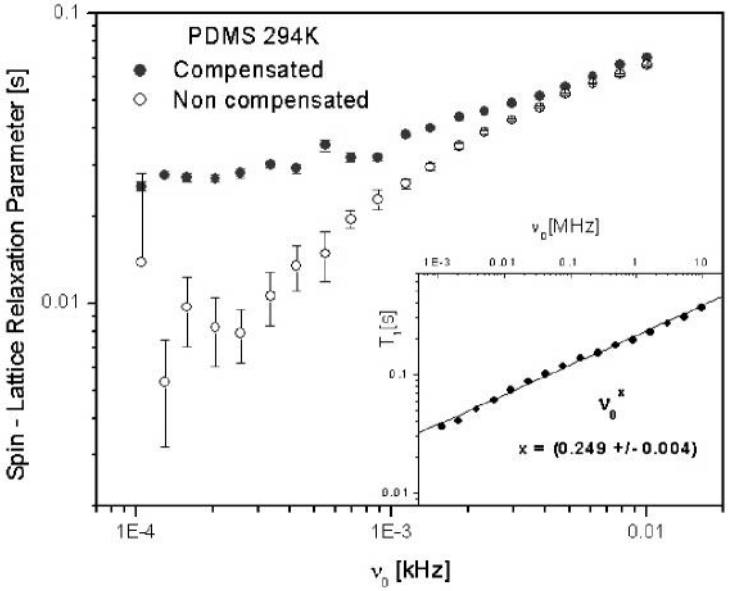

Local fields

- Plateau
- Data scattering

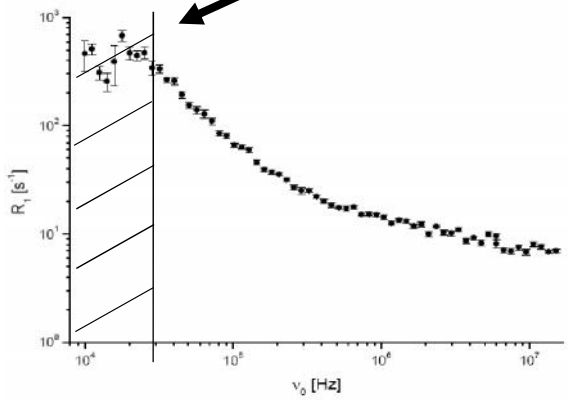

Liposomes
DMPC – D_2O 100nm

Basic literature

- F. Noack Progr. NMR Spectrosc. 18, 171 (1986).
- R. Kimmich, NMR Tomography, Diffusometry, Relaxometry. Springer. Berlin (1997).
- E. Anoardo, G. Galli and G. Ferrante, Appl. Magn. Reson. 20, 365 (2001).
- R. Kimmich and E. Anoardo, Prog. NMR Spectrosc. 44, 257 (2004).
- G. Ferrante and S. Sykora, Adv. Inorg. Chem. 57, 405 (2005).